http://doi.org/10.1093/plcell/koab315 THE PLANT CELL 2022: 34: 1289–1307

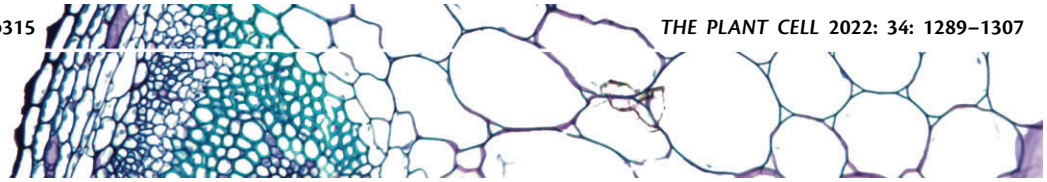

Research Article

Receptor-like cytoplasmic kinases PBL34/35/36 are required for CLE peptide-mediated signaling to maintain shoot apical meristem and root apical meristem homeostasis in Arabidopsis

Wenping Wang ,[1] Chong Hu ,[1] Xiaonan Li ,[1] Yafen Zhu ,[1] Liang Tao ,[1] Yanwei Cui ,[1] Dingqian Deng ,[1] Xiaoxuan Fan ,[1] Hong Zhang ,[1] Jia Li ,[1,2] Xiaoping Gou [1,*,†] and Jing Yi [1,*,†]

1 Ministry of Education Key Laboratory of Cell Activities and Stress Adaptations, School of Life Sciences, Lanzhou University, Lanzhou 730000, China
2 School of Life Sciences, Guangzhou University, Guangzhou 510006, China

*Author for correspondence: gouxp@lzu.edu.cn (X.G.) or yijing@lzu.edu.cn (J.Y.).
These authors contributed equally (W.W., C.H.).
†Senior authors.

W.W., C.H., X.G., and J.Y. conceived the project, designed all experiments, analyzed the data, and wrote the manuscript. X.G. and J.Y. supervised the study. W.W. and C.H. performed most of the experiments and prepared the data. X.L. and L.T. performed the RNA in situ hybridization analyses and in vivo fluorescence imaging in the SAM. Y.Z. conducted the in vitro phosphorylation assays. Y.C., D.D., X.F., and H.Z. contributed to the generation and analysis of transgenic plants and high-order mutants. J.L. helped prepare the manuscript.
The authors responsible for distribution of materials integral to the findings presented in this article in accordance with the policy described in the Instructions for Authors (https://academic.oup.com/plcell) are: Xiaoping Gou (gouxp@ lzu.edu.cn) and Jing Yi (yijing@lzu.edu.cn).

Abstract

Shoot apical meristem (SAM) and root apical meristem (RAM) homeostasis is tightly regulated by CLAVATA3 (CLV3)/EMBRYO SURROUNDING REGION-related (CLE) peptide signaling. However, the intracellular signaling components after CLV3 is perceived by the CLV1–CLV3-INSENSITIVE KINASE (CIK) receptor complex and CLE25/26/45 are sensed by the BARELY ANY MERISTEM (BAM)–CIK receptor complex are unknown. Here, we report that PBS1-LIKE34/35/36 (PBL34/35/36), a clade of receptor-like cytoplasmic kinases, are required for both CLV3-mediated signaling in the SAM and CLE25/26/45-mediated signaling in the RAM. Physiological assays showed that the SAM and RAM of *pbl34 pbl35 pbl36* were resistant to CLV3 and CLE25/26/45 treatment, respectively. Genetic analyses indicated that *pbl34 pbl35 pbl36* greatly enhanced the SAM defects of *clv2* and *rpk2* but not *clv1*, and did not show additive effects with *bam3* and *cik2* in the RAM. Further biochemical assays revealed that PBL34/35/36 interacted with CLV1, BAM1/3, and CIKs, and were phosphorylated by CLV1 and BAM1. All these results suggest that PBL34/35/36 act downstream of CLV1 and BAM1/3 to mediate the CLV3 and CLE25/26/45 signals in maintaining SAM and RAM homeostasis, respectively. Our findings shed light on how CLE signals are transmitted intracellularly after being perceived by cell surface receptor complexes.

Received September 17, 2021. Accepted December 17, 2021. Advance access publication December 22, 2021

IN A NUTSHELL

Background: Throughout their lifespans, plants continually initiate new organs. This process relies on the shoot apical meristem (SAM) and root apical meristem (RAM). SAM and RAM homeostasis is tightly regulated by CLAVATA3 (CLV3)/EMBRYO SURROUNDING REGION (ESR)-related (CLE) peptide signaling. However, we know relatively little about the intracellular signaling components after CLV3 is perceived by the CLV1–CLV3 INSENSITIVE KINASE (CIK) receptor complex and CLE25/26/45 are sensed by the BARELY ANY MERISTEM (BAM)–CIK receptor complex to modulate SAM and RAM homeostasis. Receptor-like cytoplasmic kinases (RLCKs) are the immediate signaling components acting downstream of the receptor complexes to transduce the corresponding ligand signals.

Question: We wondered whether CLV1 and BAM1/3 also need RLCKs to transduce the CLV3 and CLE25/26/45 signals in the SAM and RAM, respectively. We examined this hypothesis by disrupting the functions of a clade of RLCK genes.

Findings: Loss-of-function of *PBS1-LIKE34/35/36* (*PBL34/35/36*) resulted in enlarged SAM, more stem cells, and extra flower organs in the mutant plants. Physiological assays showed that exogenous application of CLV3 or CLE25/26/45 terminated the SAM or consumed the RAM of the wild-type plants but not the *pbl34 pbl35 pbl36* mutants. In addition, loss-of-function of *PBL34/35/36* greatly enhanced the SAM defects of *clv2* and *rpk2* but not *clv1*. Further biochemical assays revealed that PBL34/35/36 interacted with CLV1, BAM1/3, and CIKs, and were phosphorylated by CLV1 and BAM1. All these results suggested that PBL34/35/36 act downstream of CLV1 and BAM1/3 to mediate the CLV3 and CLE25/26/45 signals in maintaining SAM and RAM homeostasis, respectively.

Next steps: The *pbl34 pbl35 pbl36* mutant exhibits weaker SAM defects than *clv1*. Generating higher-order *pbl* mutants will be necessary to elucidate whether PBL34/35/36 function redundantly with their homologs or CLV1 employs distinct downstream effectors. Moreover, the downstream components of CLV signaling that directly repress *WUSCHEL* (*WUS*) expression are unknown.

Introduction

Plant cells constantly communicate with their neighboring cells, allowing normal development and responses to ever-changing environmental conditions. Peptide hormones and cell surface-localized receptor-like protein kinases (RLKs) are crucial mediators of these communications (Olsson et al., 2019). The shoot apical meristem (SAM) and root apical meristem (RAM), which are responsible for morphogenesis of the aboveground and underground plant parts, respectively, also recruit peptide–RLK receptor pairs to maintain their homeostasis (Kitagawa and Jackson, 2019).

In the SAM, the stem cell-derived peptide CLAVATA 3 (CLV3) diffuses into the organization center (OC) to repress the expression of *WUSCHEL (WUS*; Brand et al., 2000; Schoof et al., 2000). WUS, a key regulator maintaining the shoot stem cell niche, acts in a non-cell-autonomous manner to activate *CLV3* expression in a threshold-dependent manner (Perales et al., 2016; Rodriguez et al., 2016). Thus, the CLV–WUS negative-feedback loop directs the balance between cell self-renewal and cell differentiation (Somssich et al., 2016). CLV3 has been proposed to be perceived by three different receptors, including CLV1, CLV2, and RECEPTOR-LIKE PROTEIN KINASE 2 (RPK2; Clark et al., 1997; Kayes and Clark, 1998; Guo et al., 2010; Kinoshita et al., 2010). All of these receptors employ CLV3-INSENSITIVE KINASES (CIKs) as co-receptors to limit SAM size (Hu et al., 2018; Gou and Li, 2020). BARELY ANY MERISTEMS (BAMs), the homologs of CLV1, are ectopically expressed in the rib meristem (RM) in the *clv1* mutant to partially compensate for the loss-of-function of *CLV1*, indicating that BAMs and CLV1 act as redundant receptors in regulating SAM homeostasis (Deyoung and Clark, 2008; Nimchuk et al., 2015).

Genetic evidence indicates that CLV1, CLV2, and RPK2 act in three parallel pathways transducing the CLV3 signal to regulate SAM homeostasis, implying that these three receptors may employ different downstream components to transduce the CLV3 signal into the cytoplasm (Kinoshita et al., 2010). CORYNE (CRN), a receptor-like cytoplasmic kinase (RLCK) that lacks an extracellular domain (Müller et al., 2008), can interact with CLV2, a leucine-rich repeat receptor-like protein (LRR-RLP), via their transmembrane domains to form a complex (Bleckmann et al., 2010). The loss-of-function of *CRN* can strongly enhance the SAM defects of *clv1* and *rpk2*, but not *clv2*, indicating that CRN specifically functions in the CLV2 pathway (Müller et al., 2008). Heterotrimeric G proteins play key roles in transmitting signals from RLK receptors into the cytoplasm (Pandey, 2019). Additional mutations of GTP BINDING PROTEIN BETA 1 (AGB1, Gβ) or ARABIDOPSIS G-PROTEIN GAMMA-SUBUNIT 1/2 (AGG1/2, Gγ) do not alter SAM defects of the *rpk2* mutant, but significantly enhance the SAM defects of *clv1* and *clv2*. Further biochemical evidence shows that AGB1 physically interacts with RPK2. Therefore, it was proposed that Gβγ and RPK2 regulate SAM maintenance through a common pathway (Ishida et al., 2014). However, the immediate events after CLV3 is recognized by the CLV1–CIK complex are not clear in Arabidopsis.

The CLV–WUS feedback signaling pathway appears to be conserved across angiosperms (Somssich et al., 2016). Maize (*Zea mays*) THICK TASSEL DWARF 1 (TD1) and

FASCIATED EAR 2 (FEA2) are orthologs of Arabidopsis CLV1 and CLV2 (Taguchi-Shiobara et al., 2001; Bommert et al., 2005). FEA3, another LRR-RLP, is expressed in the central region of the SAM to perceive ZmFON2-LIKE CLE PROTEIN 1 (ZmFCP1), the CLV3 ortholog in maize, to regulate SAM homeostasis (Je et al., 2016). Similar to CLV1 and CLV2 in Arabidopsis, TD1 functions in parallel with FEA2 and FEA3 in maize (Je et al., 2016). FEA2 also employs ZmCRN as a downstream effector transducing the ZmFCP1 signal to regulate stem cell niche in maize (Je et al., 2018). Interestingly, maize COMPACT PLANT 2 (CT2, Gα) and ZmGB1 (Gβ) also act downstream of FEA2 to maintain SAM homeostasis by perceiving ZmCLE7, another CLV3 ortholog in maize (Bommert et al., 2013b; Wu et al., 2020). The downstream module of TD1 in maize is still undiscovered.

In addition to the aforementioned regulators, several other essential components involved in stem cell maintenance have been identified. POLTERGEIST (POL) and POL-Like 1 (PLL1), two PP2C phosphatases, function upstream of WUS as negative regulators in the CLV3 signaling pathway. The loss-of-function of POL and PLL1 suppresses SAM defects of the weak *clv1* and *clv2* mutants, and the *pol pll1* double mutant shows phenotypes similar to the *wus* mutant (Song and Clark, 2005; Song et al., 2006). A recent work showed that POL and PLLs directly interact with and dephosphorylate CLV1 and BAMs (DeFalco et al., 2021). Mitogen-activated protein kinase (MAPK) cascades, which have been proposed to mediate multiple RLK signals in the cytoplasm (Wang and Gou, 2020), are also involved in CLV3-mediated SAM regulation (Betsuyaku et al., 2011b). The CLV3-activated phosphorylation of MPK3 and MPK6 is dependent on CLV1 and BAM1. In addition, the SAM of a conditional *mpk3 mpk6* double mutant is insensitive to CLV3 treatment (Lee et al., 2019). However, the MAPK kinases (MKKs) and MKK kinases (MKKKs) acting upstream of MPK3/6, and the signaling elements connecting MKKKs and CLV1/BAM1 receptors in the SAM need further investigation.

Besides functioning in the SAM, CLE peptide-triggered signaling is also crucial for RAM homeostasis. Exogenous applications of Groups A and B CLEs greatly decrease the activity of the proximal root meristem (Ito et al., 2006; Betsuyaku et al., 2011a), possibly due to the suppression of protophloem differentiation (Depuydt et al., 2013; Hazak et al., 2017). Furthermore, many key regulators in the SAM also exhibit conserved functions in the proximal root meristem (Zhu et al., 2020). BAM1/3, the homologs of CLV1, and CIKs form a receptor complex in a ligand-induced manner to regulate CLE25/26/45-mediated suppression of protophloem differentiation and consumption of the proximal root meristem (Depuydt et al., 2013; Anne et al., 2018; Ren et al., 2019; Hu et al., 2022). In addition, CLV2/CRN, a heteromer of CLV2 and CRN, and RPK2 are involved in CLE signaling to regulate homeostasis of the proximal root meristem (Fiers et al., 2005; Müller et al., 2008; Bleckmann et al., 2010; Kinoshita et al., 2010; Gujas et al., 2020). RPK2 also forms a heteromeric complex with BAM1, which is involved in CLE peptide-dependent shrinkage of the proximal root meristem (Shimizu et al., 2015). Although several receptors have been demonstrated to mediate CLE signaling in the RAM, more signaling elements that directly interact with these receptors to transmit the signals into the cytoplasm have not been characterized yet.

To date, it has been revealed that RLCKs are employed as the immediate signaling components acting downstream of RLKs to transduce the corresponding ligand signals. For example, CONSTITUTIVE DIFFERENTIAL GROWTH 1 (CDG1) and the BRASSINOSTEROID (BR)-SIGNALING KINASE (BSK) family members are phosphorylated by BRASSINOSTEROID-INSENSITIVE 1 (BRI1), an LRR type RLK functioning as a major BR receptor, to modulate BR signaling (Tang et al., 2008; Kim et al., 2011; Sreeramulu et al., 2013); BOTRYTIS-INDUCED KINASE1 (BIK1) and its homolog PBS1-LIKE 1 (PBL1) directly interact with various pattern recognition receptors, such as FLAGELLIN SENSING 2 (FLS2), ELONGATION FACTOR-TU (EF-Tu) RECEPTOR (EFR), PEP RECEPTORs (PEPRs), and LYSINE MOTIF RECEPTOR KINASE 5 (LYK5), to regulate plant innate immune responses (Lu et al., 2010a; Zhang et al., 2010; Liu et al., 2013; Kadota et al., 2014; Ranf et al., 2014); RPM1-INDUCED PROTEIN KINASE (RIPK) is required for RAPID ALKALINIZATION FACTOR 1 (RALF1) signaling and functions downstream of FERONIA (FER) to regulate primary root and root hair growth (Du et al., 2016); MARIS (MRI) acts as a key downstream component of ANXUR 1/2 (ANX1/2) and FER to monitor cell wall integrity in pollen tube and root hair (Boisson-Dernier et al., 2015; Liao et al., 2016); CAST AWAY (CST) interacts with both HAESA (HAE) and SUPPRESSOR OF BIR 1 (SOBIR1)/EVERSHED (EVR) to inhibit organ abscission (Burr et al., 2011). It has been accepted as a paradigm that RLK-regulated biological processes require RLCKs to transduce the corresponding signals to downstream signaling components (Liang and Zhou, 2018). However, whether CLV1 and BAM1/3 also need RLCKs to transduce the CLV3 and CLE25/26/45 signals in the SAM and RAM has not been elucidated.

Here, we report that PBL34/35/36, three members of the RLCK VII subfamily required for LIPOOLIGOSACCHARIDE-SPECIFIC REDUCED ELICITATION (LORE)-mediated plant immunity regulation (Luo et al., 2020), play key roles in CLV3-mediated SAM regulation and CLE25/26/45-mediated RAM regulation through acting directly downstream of CLV1 and BAM1/3, respectively. The root length and protophloem of *pbl34 pbl35 pbl36* show resistance to CLE45 treatment, which is similar to observations for *bam3* and *cik2* (Depuydt et al., 2013; Anne et al., 2018; Ren et al., 2019). Moreover, the *pbl34 pbl35 pbl36* triple mutants generate enlarged SAMs and extra flower organs, similar to those observed for *clv1* (Clark et al., 1997). The loss-of-function of *PBL34/35/36* greatly enhances the SAM defects of *clv2* and *rpk2*, but not *clv1*. Furthermore, PBL34/35/36 can interact with CLV1, BAM1/3, and CIKs both in vivo and in vitro, and

can be phosphorylated by CLV1 and BAM1 in vitro. Our studies reveal that PBL34/35/36 act as conserved regulators downstream of CLV1 and BAM1/3 to maintain homeostasis of both the SAM and RAM.

Results

PBL34 may sense CLE45 to regulate root growth

Increasing lines of evidence indicate that RLCKs act as direct components downstream of RLKs to regulate diverse biological processes (Liang and Zhou, 2018), implying that CLV1-mediated SAM homeostasis and BAM1/3-mediated RAM homeostasis may need such RLCKs as well. There are 149 RLCKs that were divided into 17 subgroups based on their sequence homology in Arabidopsis (Shiu et al., 2004). Although the functions of most RLCKs have not been elucidated, some members of the RLCK VII subfamily have been clarified to be involved in plant immunity and development. Several of them act downstream of RLKs to transduce peptide signals including INFLORESCENCE DEFICIENT IN ABSCISSION (IDA; Burr et al., 2011), whose mature peptide is similar to CLE (Zhang et al., 2020). We wondered whether the RLCK VII subfamily members are also required for CLE peptide signaling.

To this end, 28 homozygous T-DNA insertion lines of the RLCK VII subfamily genes were treated with 20-nM CLE45 on half-strength Murashige–Skoog (MS) medium, and the primary root length was examined at 5 days after germination. We found that the relative root length of *pbl34* was significantly longer than that of other *rlck vii* mutants upon 20-nM CLE45 treatment. To further confirm that *pbl34* was resistant to CLE45, different concentrations of CLE45 were applied to *pbl34* seedlings. Root growth of the *pbl34* single mutant was also less sensitive than the wild-type control to treatment with 100-nM CLE45, indicating that PBL34 may be involved in CLE45 signaling to regulate root growth (Supplemental Figure S1A).

PBL34/35/36 function redundantly to sense root-active CLE peptides

Despite the root of *pbl34* seedlings being less sensitive than the wild-type control to CLE45, the treatment still resulted in significantly shortened *pbl34* root when compared with the mock treatment (Supplemental Figure S1A), indicating that CLE45 signaling was partially retained in the *pbl34* mutant and the homologs of PBL34 may function redundantly to regulate root growth. PBL34 belongs to the RLCK VII-5 subclade that contains two homologs PBL35 and PBL36 (Supplemental Figure S1B and Supplemental Data Set S1; Rao et al., 2018).

To explore the potential functional redundancy of PBL35 and PBL36 with PBL34 in CLE45 signaling, we examined the expression patterns of these *PBLs* in the RAM using the *ProPBL:gPBL-YFP* reporter lines. *PBL34* is mainly expressed in the stem cell niche and stele in the RAM; *PBL35* is mainly expressed in the proximal root meristem, and *PBL36* is ubiquitously expressed throughout the RAM (Supplemental Figure S2). Taken together, all three *PBL* genes are expressed in the RAM, indicating that they may function redundantly to regulate the proximal root meristem.

Therefore, the *pbl34 pbl36* and *pbl35 pbl36* double mutants and three independent *pbl34 pbl35 pbl36* triple mutants (Supplemental Figure S3) were generated by genetic cross or clustered regularly interspaced short palindromic repeats (CRISPR)/CRISPR-associate protein 9 (Cas9)-based gene editing for analyzing their responses to CLE treatment. The wild-type plants grown on 1/2 MS medium with 100-nM CLE25 or CLE45 showed significantly shortened roots with a decreased proximal root meristem (Figure 1; Supplemental Figures S1A and S4). When treated with CLE45, the *pbl34 pbl36* and *pbl35 pbl36* double mutants showed reduced sensitivity than the wild-type control, which was similar to that of *pbl34*, while the *pbl34 pbl35 pbl36-1* (hereafter named *pbl34 pbl35 pbl36* for brevity) triple mutants were less sensitive than the other *pbl* mutants tested (Supplemental Figure S1A), suggesting that PBL34, PBL35, and PBL36 function redundantly to sense CLE signals in regulating root growth and maintaining the proximal root meristem, and that PBL34 plays the most important role in this process. Two other independent *pbl34 pbl35 pbl36* triple mutants showed similarly reduced sensitivity when treated with 100-nM CLE25 or CLE45 (Figure 1; Supplemental Figure S4). The complementation of *pbl34 pbl35 pbl36-2* by *PBL34*, *PBL35*, and *PBL36* under a *UBQ10* promoter further confirmed that PBL34/35/36 function in CLE-mediated proximal root meristem maintenance and root growth (Supplemental Figure S5A).

As BAM1/3 and CIKs are required for the sensing of all root-active CLE peptides (Figure 1; Anne et al., 2018; Hu et al., 2018, 2022), which prompted us to investigate whether PBL34/35/36 are also required for the sensing of various CLEs. The results showed that the *pbl34 pbl35 pbl36* mutants were not only partially resistant to CLE45, but also partially resistant to all the root-active CLE peptides (Supplemental Figure S6). Taken together, these data demonstrate that PBL34/35/36 function redundantly to regulate CLE-mediated proximal root meristem maintenance.

PBL34/35/36 are required for CLE-mediated suppression of protophloem differentiation in the root

Exogenous application of CLE peptides suppresses the differentiation of protophloem to affect maintenance of the proximal root meristem (Hazak et al., 2017). Protophloem precursor cell differentiation is associated with a thickening of the protophloem cell wall, which can be strongly stained by propidium iodide (PI; Truernit et al., 2008). When the wild-type seedlings were treated with CLE45, the typical cell wall staining of the protophloem cells was abolished. However, the strongly stained cells were clearly observed in almost all roots of *pbl34 pbl35 pbl36* (Figure 2, A–D), suggesting that the protophloem cells can be properly differentiated upon CLE45 treatment when the PBL34/35/36-mediated signaling is blocked.

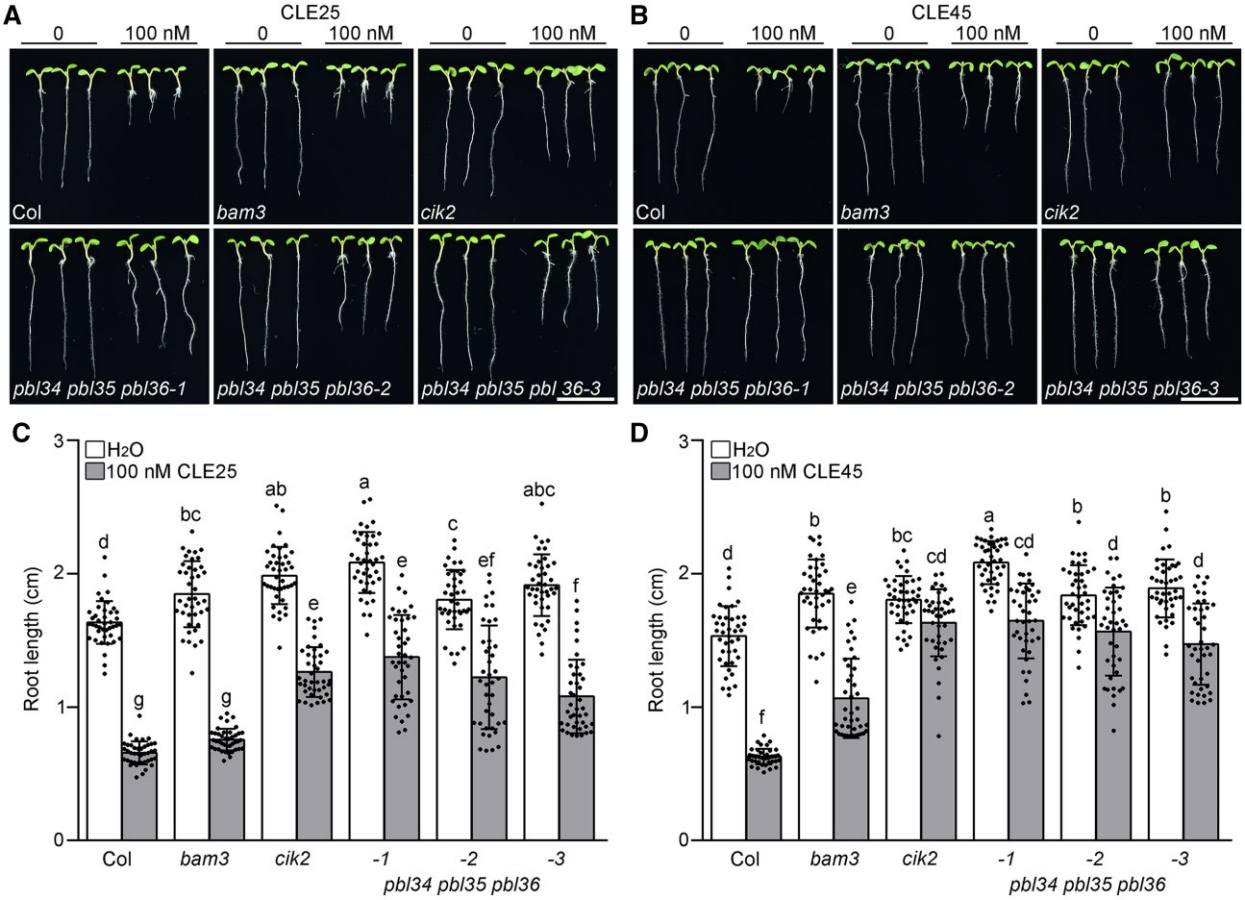

Figure 1 *PBL34/35/36* are required for sensing CLE25 and CLE45. A, B, Five-day-old seedlings of Col, *bam3*, *cik2*, *pbl34 pbl35 pbl36-1*, *pbl34 pbl35 pbl36-2*, and *pbl34 pbl35 pbl36-3* grown on 1/2 MS medium with 0-nM, 100-nM CLE25 (A) or CLE45 (B) peptide. Roots of *cik2*, *pbl34 pbl35 pbl36-1*, *pbl34 pbl35 pbl36-2*, and *pbl34 pbl35 pbl36-3* showed reduced sensitivity to CLE25 or CLE45 when compared with the wild-type plants. Scale bar: 1 cm. C, D, Quantitative analyses of root length of the indicated genotypes under the conditions shown in (A) and (B). Data are shown as mean ± SD ($n \geqslant 40$). Different lowercase letters indicate statistically significant differences based on two-way analysis of variance (ANOVA) with Tukey's multiple comparisons test ($P < 0.05$).

To further confirm that the protophloem is still retained in the *pbl34 pbl35 pbl36* mutants, promoters of *COTYLEDON VASCULAR PATTERN 2* (*CVP2*; Rodriguez-Villalon et al., 2015) and *ALTERED PHLOEM DEVELOPMENT* (*APL*; Bonke et al., 2003), two protophloem markers, were cloned to drive the expression of a nuclear-localized yellow fluorescent protein (YFP) in the wild-type and *pbl34 pbl35 pbl36* mutant background. Interestingly, *CVP2* was expressed earlier in the *pbl34 pbl35 pbl36* mutants than in the wild-type plants, indicating that the protophloem differentiation may be premature in *pbl34 pbl35 pbl36* (Figure 2, E, G, M, and N). Consistent with the previous results, the expression of *CVP2* and *APL* was not detected in the wild-type plants upon CLE45 treatment, while the fluorescence signal was still observed in the *pbl34 pbl35 pbl36* mutants upon CLE45 treatment (Figure 2, E–L), indicating that PBL34/35/36 are essential for CLE45-mediated suppression of protophloem differentiation. Although *CVP2* and *APL* are still expressed in the *pbl34 pbl35 pbl36* mutants upon CLE45 treatment, the distance between cells with *CVP2* or *APL* expression and the quiescent center (QC) is markedly farther (Figure 2, E–N). These results suggest that CLE signaling is greatly impaired but not completely blocked in the *pbl34 pbl35 pbl36* mutants. It is possible that, besides PBL34/35/36, other PBL homologs can partially compensate for the loss-of-function of PBL34/35/36.

PBL34/35/36 act in the CLE–BAM–CIK signaling pathway to regulate proximal root meristem homeostasis

It was reported that the CLE–BAM–CIK signaling module is involved in regulating protophloem differentiation and proximal root meristem (Hu et al., 2022). As described above, since PBL34/35/36 are required for CLE sensing, we wondered whether PBL34/35/36 act in the same genetic pathway with BAM–CIK. Therefore, we compared the CLE resistances of *bam3 pbl34 pbl35 pbl36* with *bam3* and *pbl34 pbl35 pbl36*, and *cik2 pbl34 pbl35 pbl36* with *cik2* and *pbl34 pbl35 pbl36*. The results showed that *bam3 pbl34 pbl35 pbl36* and *cik2 pbl34 pbl35 pbl36* did not show significantly additive effects when compared with the corresponding single mutants and *pbl34 pbl35 pbl36*, suggesting that

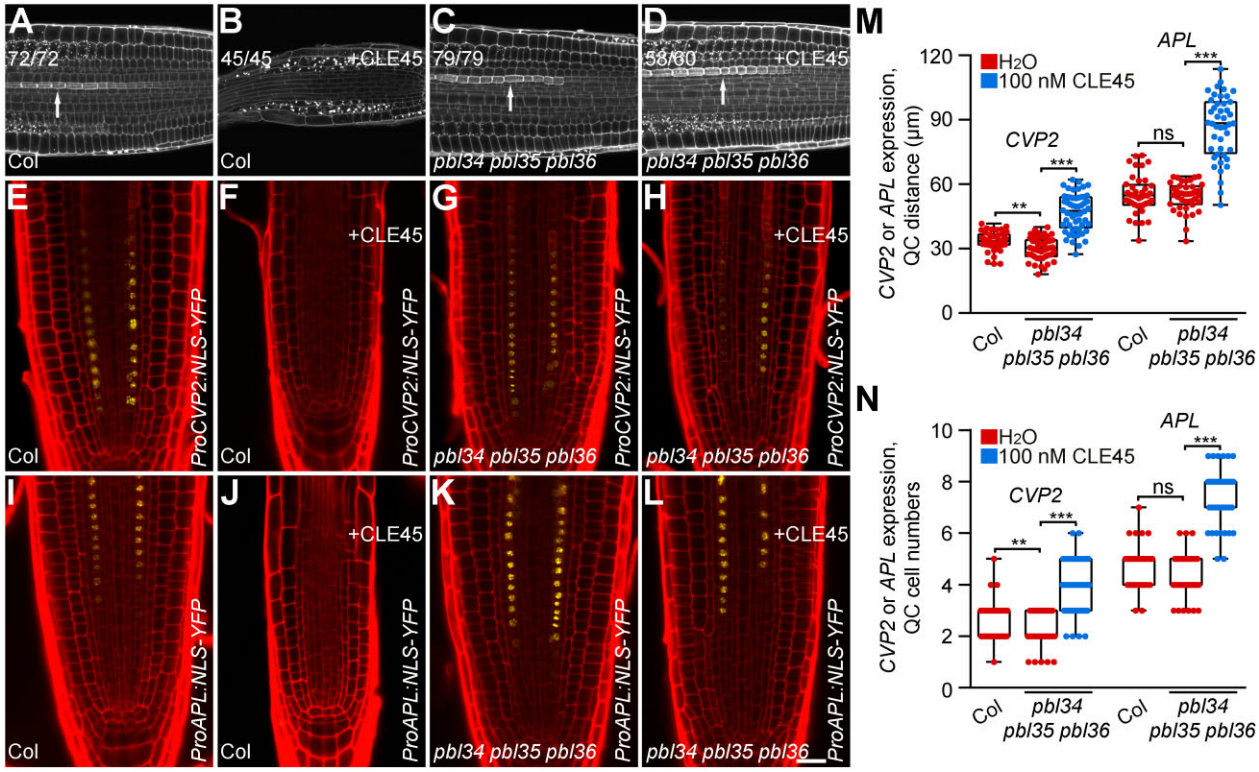

Figure 2 *PBL34/35/36* are required for CLE45-mediated suppression of protophloem differentiation. A–D, The protophloem of 5-day-old seedlings was analyzed by mPS-PI staining. Representative roots of Col (A and B) and *pbl34 pbl35 pbl36* (C and D) grown on 1/2 MS medium without (A and C) or with (B and D) 100-nM CLE45 peptide are shown. E–L, Expression of *CVP2* and *APL* was detected by *ProCVP2:NLS-YFP* and *ProAPL:NLS-YFP* reporter lines, respectively, in Col (E, F, I, and J) and *pbl34 pbl35 pbl36* (G, H, K, and L) treated with (F, H, J, and L) or without (E, G, I, and K) 100-nM CLE45. The YFP fluorescence signals (yellow) in 5-day-old seedlings were observed using confocal laser scanning microscopy after PI staining (red). Scale bar: 50 μm. M and N, Quantitative analyses of the distance and cell number between the first cell with detectable *CVP2* or *APL* expression and the QC position in the indicated genotypes. Box limits indicate 25th and 75th percentiles; horizontal line is the median; whiskers display minimum and maximum values. Dots represent individual measurements from more than 40 samples per group. $^{***}P < 0.001$, $^{**}P < 0.01$, ns represents no significant difference (two-tailed Student's *t* test).

PBL34/35/36 might act in the same pathway with BAM–CIK (Supplemental Figure S7).

BREVIS RADIX (BRX) and OCTOPUS (OPS) have been reported to be required for proper differentiation of protophloem and maintenance of the proximal root meristem (Truernit et al., 2012; Rodriguez-Villalon et al., 2014). The short-root phenotype of *brx* and *ops*, which may be due to the amplified CLE signaling, can be largely rescued by *bam3* and *cik2 cik3 cik4 cik5 cik6* (Depuydt et al., 2013; Rodriguez-Villalon et al., 2014; Breda et al., 2019; Hu et al., 2022). To further investigate the roles of PBL34/35/36 in CLE25/26/45 signaling, additional genetic analyses were carried out to elucidate whether PBL34/35/36 function together with BRX and OPS. The results showed that *pbl34 pbl35 pbl36* partially rescued the short-root phenotype of *brx* and *ops* since the *brx pbl34 pbl35 pbl36* and *ops pbl34 pbl35 pbl36* quadruple mutants exhibited roots that were slightly longer than those of the *brx* and *ops* mutants (Supplemental Figure S8), suggesting that PBL34/35/36 may be involved in BRX and OPS signaling. It is notable that the *bam3* and *cik2 cik3 cik4 cik5 cik6* mutations can greatly rescue the short-root phenotype of the *brx* and *ops* mutants (Depuydt et al., 2013; Rodriguez-Villalon et al., 2014), which is similar to but more significant than the effect of the *pbl34 pbl35 pbl36* triple mutant, suggesting that additional homologs of PBL34/35/36 may still function to mediate the root-active CLE signals. Taken together, these results suggest that PBL34/35/36, possibly with their homologs, may function in the BAM–CIK signaling pathway to regulate the proximal root meristem.

SAM homeostasis is disturbed in the *pbl34 pbl35 pbl36* mutant

It was reported that SAM and RAM share many common or similar regulators to maintain their homeostasis (Zhu et al., 2020). To explore whether PBL34/35/36 also regulate SAM homeostasis, we first detected the expression patterns of *PBL34/35/36* in the SAM using the *ProPBL:gPBL-YFP* reporter lines. The fluorescent reporters revealed that *PBL34/35/36* are widely expressed in the inflorescence, including the inflorescence meristems (IMs), flower primordia, and flower meristems. In the IM, *PBL34/35/36* are expressed in the central zone (CZ), peripheral zone, and OC (Supplemental Figure S9), overlapping with the expression of *CLV1* and *CIKs* (Hu et al., 2018; Blümke et al., 2021).

We therefore examined the SAM size, IM morphology, and carpel numbers of the *pbl34 pbl35 pbl36* mutants. Results showed that the SAM heights of three independent *pbl34 pbl35 pbl36* triple mutants are slightly greater than those of the wild-type plants, and the SAM widths are indistinguishable from those of the wild-type plants (Figure 3, A–D, I, and J). Although the IM morphology is not strongly disturbed in the *pbl34 pbl35 pbl36* mutants (Figure 3, E–H), three independent *pbl34 pbl35 pbl36* triple mutants develop flowers with increased numbers of carpels relative to the wild-type flower, which produces two carpels. Reintroduction of *PBL34*, *PBL35*, and *PBL36* into the *pbl34 pbl35 pbl36-2* mutants can completely suppress the extra carpels of the *pbl34 pbl35 pbl36-2* mutants (Supplemental Figure S5B). Interestingly, siliques at the top part of the inflorescence have more carpels than those at the basal part (Figure 3K) indicating that SAM homeostasis is disrupted and the defects are enhanced over time in the *pbl34 pbl35 pbl36* mutants.

To further confirm that SAM homeostasis is disrupted in the *pbl34 pbl35 pbl36* mutants, the expression patterns of *CLV3* and *WUS*, two marker genes expressed in the stem cells and OC of the SAM, respectively, were analyzed by RNA in situ hybridization. In the wild-type plants, *CLV3* is exclusively expressed as a small triangle in the CZ. However, the expression domain of *CLV3* is obviously expanded in the SAM in all three independent *pbl34 pbl35 pbl36* triple mutants. The expression levels of *CLV3* are also dramatically increased in the *pbl34 pbl35 pbl36* mutants (Figure 4, A–D). In the wild-type plants, *WUS* is expressed in a small group of cells (11.1 ± 1.2, $n = 8$). In the *pbl34 pbl35 pbl36* mutants, the expression of *WUS* is markedly expanded into more cells (17 ± 2.5, $n = 7$), although the expression level is not significantly increased (Figure 4, E–H). These SAM defects in the

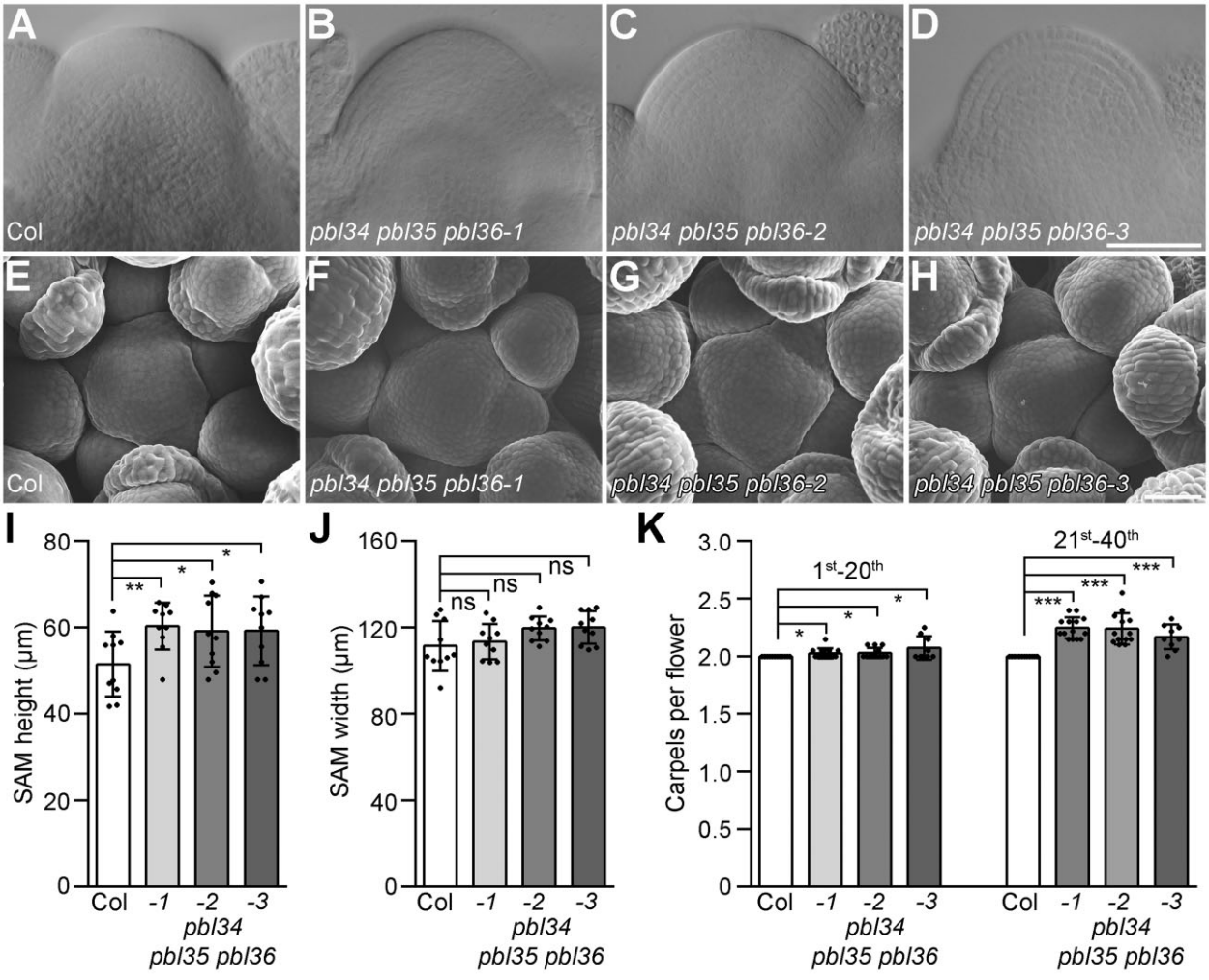

Figure 3 The *pbl34 pbl35 pbl36* triple mutant shows an enlarged SAM. A–D, DIC images of SAM from 19-day-old seedlings of Col (A), *pbl34 pbl35 pbl36-1* (B), *pbl34 pbl35 pbl36-2* (C), and *pbl34 pbl35 pbl36-3* (D). Scale bar: 50 μm. E–H, SEM images of 5-week-old IM in Col (E), *pbl34 pbl35 pbl36-1* (F), *pbl34 pbl35 pbl36-2* (G), and *pbl34 pbl35 pbl36-3* (H). Scale bar: 50 μm. I–K, Quantitative analysis of SAM height (I), width (J), and carpel number in the 1st–20th and 21st–40th siliques (K). Data are shown as mean ± SD (n = 10 independent plants, each sample represents the average carpel number of the first (left) or second (right) 20 siliques of each plant.). ***$P < 0.001$, **$P < 0.01$, *$P < 0.05$, ns represents no significant difference (two-tailed Student's t test).

pbl34 pbl35 pbl36 mutants, including enlarged SAM, siliques with extra carpels, and enhanced and expanded expression of *CLV3* and *WUS*, are reminiscent of the *clv* mutants (Clark et al., 1997; Kayes and Clark, 1998), suggesting that the CLV–WUS negative-feedback loop is disrupted in the *pbl34 pbl35 pbl36* mutant.

PBL34/35/36 are involved in the CLV3–WUS pathway to maintain SAM homeostasis

The above results indicated that PBL34/35/36 are involved in regulating SAM homeostasis possibly through the CLV–WUS pathway. Since PBL34/35/36 are members of the RLCK family, they may be involved in sensing the CLV3 signal in the SAM. Therefore, both the wild-type plants and the *pbl34 pbl35 pbl36* mutants were treated with 5-μM synthesized CLV3 to examine their sensitivities. Consistent with previous reports, the wild-type seedlings displayed terminated SAMs and did not generate inflorescence stems when they were grown on MS medium containing 5-μM CLV3 for 4 weeks. However, about 60% of the *pbl34 pbl35 pbl36* mutants still retained the SAM and generated an inflorescence stem under the same growth conditions (Figure 4, I–L; Supplemental Figure S10). To elucidate the differential contributions of each PBL for maintaining SAM homeostasis, all single and double mutants of *PBL34/35/36* were further examined to analyze their sensitivities to CLV3. The results showed that all single mutants exhibited responses similar to the wild-type plants, while about 3% of the *pbl35 pbl36* mutants, 6% of the *pbl34 pbl36* mutants, and 24% of the *pbl34 pbl35* mutants exhibited resistance to CLV3 treatment and generated inflorescence stems (Supplemental Figure S10). Taken together, these results demonstrate that PBL34/35/36 are redundantly required for CLV3-mediated SAM homeostasis, and that PBL34 may play a major role in this process.

WUS, which acts downstream of CLV3, is necessary and sufficient to determine stem cell identity (Gallois et al., 2004). Disruption of *WUS* function leads to the loss of stem cells in the SAM (Mayer et al., 1998). To determine the genetic relationship between *PBL34/35/36* and *WUS*, a *wus pbl34 pbl35 pbl36* quadruple mutant was generated to examine its phenotypes in the meristem. We found that the *wus pbl34 pbl35 pbl36* mutant exhibits premature meristem termination, which is similar to the *wus* mutant (Figure 4, M–P), suggesting that *PBL34/35/36* act upstream of *WUS* to maintain SAM homeostasis.

PBL34/35/36 function in the CLV1 pathway to regulate SAM homeostasis

It has been demonstrated that the CLV3 signal is transduced by three parallel pathways mediated by CLV1, CLV2/CRN, and RPK2 to maintain SAM homeostasis (Clark et al., 1997; Kayes and Clark, 1998; Müller et al., 2008; Kinoshita et al., 2010; Kitagawa and Jackson, 2019). Our results suggest that PBL34/35/36 are involved in CLV3-mediated SAM regulation. To investigate whether PBL34/35/36 are required by these three signaling pathways to regulate SAM homeostasis, we created the quadruple mutants *clv1 pbl34 pbl35 pbl36*, *clv2 pbl34 pbl35 pbl36*, and triple mutant *rpk2 pbl34 pbl36* due to the genetic linkage between *RPK2* and *PBL35*, to examine the SAM-related phenotypes. Surprisingly, rosettes of the *clv1 pbl34 pbl35 pbl36* quadruple mutants do not display significant morphological alterations when compared with those of *pbl34 pbl35 pbl36* and *clv1* (Supplemental Figure S11, B, E, and F). In addition, the *clv1 pbl34 pbl35 pbl36* quadruple mutant and the *clv1* single mutant show discontinuous flower outgrowth indistinguishable from each other (Supplemental Figure S11, J and N). However, the *clv2 pbl34 pbl35 pbl36* and *rpk2 pbl34 pbl36* mutants produce significantly more rosette leaves when compared with *clv2* and *rpk2*, respectively (Supplemental Figure S11, C, D, G, and H). Moreover, the *clv2 pbl34 pbl35 pbl36* quadruple mutants produce a fasciated inflorescence stem with many more flowers than the *clv2* and *pbl34 pbl35 pbl36* mutants (Supplemental Figure S11, K, M, and O). The *rpk2 pbl34 pbl36* mutant displays a discontinuous flower outgrowth, which resembles that of *clv1* and is much more severe than that of the *rpk2* and *pbl34 pbl35 pbl36* mutants (Supplemental Figure S11, L, M, and P).

The SAMs of *clv1 pbl34 pbl35 pbl36*, *clv2 pbl34 pbl35*, and *rpk2 pbl34 pbl36* were further analyzed. The results showed that the SAM of *clv1 pbl34 pbl35 pbl36* is higher than that of the wild-type and the *pbl34 pbl35 pbl36* mutant, but is indistinguishable from that of the *clv1* mutant (Figure 5, A, B, F, and I). Due to the extremely irregular SAM of *clv2 pbl34 pbl35 pbl36*, the SAM of the *clv2 pbl34 pbl35* triple mutant was analyzed. Both *clv2 pbl34 pbl35* and *rpk2 pbl34 pbl36* generate a significantly higher SAM when compared with the corresponding single mutants *clv2* and *rpk2*, and the *pbl34 pbl35 pbl36* triple mutant, respectively (Figure 5, C, D, and G–I). To further confirm the genetic effect of *pbl34 pbl35 pbl36* in the *clv1*, *clv2*, and *rpk2* background, we analyzed the IM morphology, carpel number, and *CLV3* expression level of these mutants. The results showed that the *clv1 pbl34 pbl35 pbl36* mutant produces an enlarged IM, which is similar to that of *clv1* (Figure 6, B and F). In addition, *clv1 pbl34 pbl35 pbl36* and *clv1* produce siliques with similar carpel numbers (Figure 6I). Consistent with the higher vegetative SAM than *clv2*, *clv2 pbl34 pbl35 pbl36* exhibits a dramatically enlarged irregular IM and significantly increased carpel numbers when compared with the *clv2* single mutant (Figure 6, C, G, and I). Similarly, *rpk2 pbl34 pbl36* also shows an enlarged IM and significantly increased carpel numbers when compared with the *rpk2* single mutant (Figure 6, D, H, and I). Consistent with the IM size, the *CLV3* expression level in the inflorescence of *clv1 pbl34 pbl35 pbl36* is just slightly upregulated when compared with *clv1*, whereas both *clv2 pbl34 pbl35 pbl36* and *rpk2 pbl34 pbl36* exhibit more than 40-fold upregulated expression of *CLV3* when compared with *clv2* and *rpk2*, respectively (Figure 6J).

Taken together, these data indicate that mutations of *PBL34/35/36* cannot enhance the SAM defects of *clv1*, but

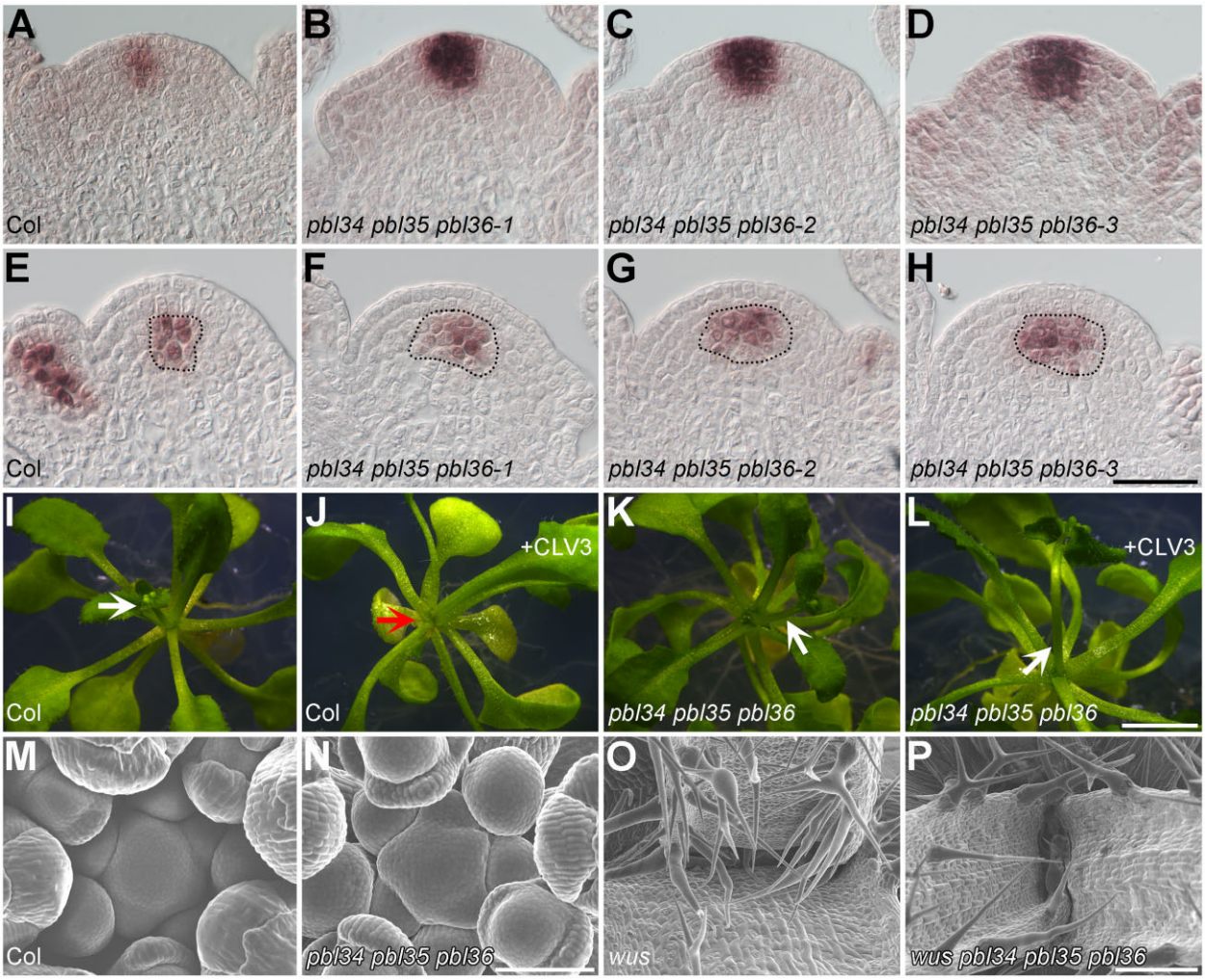

Figure 4 *PBL34/35/36* function in the CLV3-WUS pathway to maintain SAM homeostasis. A–H, RNA in situ hybridization showing the expression patterns of *CLV3* (A–D) and *WUS* (E–H) in the IMs of Col (A and E), *pbl34 pbl35 pbl36-1* (B and F), *pbl34 pbl35 pbl36-2* (C and G), and *pbl34 pbl35 pbl36-3* (D and H). Scale bar: 30 μm. The cells that were marked by antisense probe of *WUS* are indicated with dotted black lines. I–L, Four-week-old seedlings of Col (I and J) and *pbl34 pbl35 pbl36* (K and L) grown on MS medium without (I and K) or with (J and L) 5 μM CLV3. Scale bar: 5 mm. White arrows indicate the bolting inflorescence stem, and the red arrow indicates the terminated SAM. M–P, SEM images of 30-day-old SAMs from Col (M), *pbl34 pbl35 pbl36* (N), *wus* (O), and *wus pbl34 pbl35 pbl36* (P). Scale bars: 100 μm (M and N) and 500 μm (O and P).

greatly enhance the SAM defects of *clv2* and *rpk2*. In other words, our genetic data suggest that PBL34/35/36 may function in the CLV1 signaling pathway, and possibly act parallel to CLV2/CRN and RPK2 in mediating the CLV3 signal for maintaining SAM homeostasis.

PBL34/35/36 interact with CLV1, BAM1/3, and CIKs

Our results strongly indicate that PBL34/35/36 play roles in both CLE-mediated signaling in the proximal root meristem and CLV3-mediated signaling in the SAM. In addition, the genetic data suggest that PBL34/35/36 act together with BAM3 and CIK2 to sense CLE45 in the RAM (Supplemental Figure S7), and act together with CLV1 to transduce the CLV3 signal in the SAM (Figures 5 and 6). On the other hand, CIKs have been shown to function as coreceptors of CLV1 and BAMs in both the SAM and RAM (Hu et al., 2018, 2022). Therefore, we next investigated whether PBL34/35/36 can interact with CLV1, BAMs, and CIKs. Results of yeast two-hybrid analysis demonstrated that PBL34/35/36 can interact with CLV1, BAM3, CIK1, and CIK2, but not SOBIR1 (Supplemental Figure S12A). A split YFP-based bimolecular fluorescence complementation (BiFC) assay also confirmed the interactions between PBL34/35/36 and CLV1, BAM1, BAM3, CIK1, and CIK2 (Figure 7A). Consistent with the genetic results, PBL34/35/36 did not interact with CLV2, which is different from CRN, indicating that PBL34/35/36 may act in parallel with CLV2/CRN. After isolating mesophyll protoplasts of *Nicotiana benthamiana*, these interactions were shown to occur at the plasma membrane, which is consistent with the notion that these proteins are membrane-localized (Supplemental Figure S12B). Moreover, the fluorescence resonance energy transfer (FRET) assays between PBL34/35 and CLV1, BAM3, or CIK1/2 were performed with inducible expression, and the results

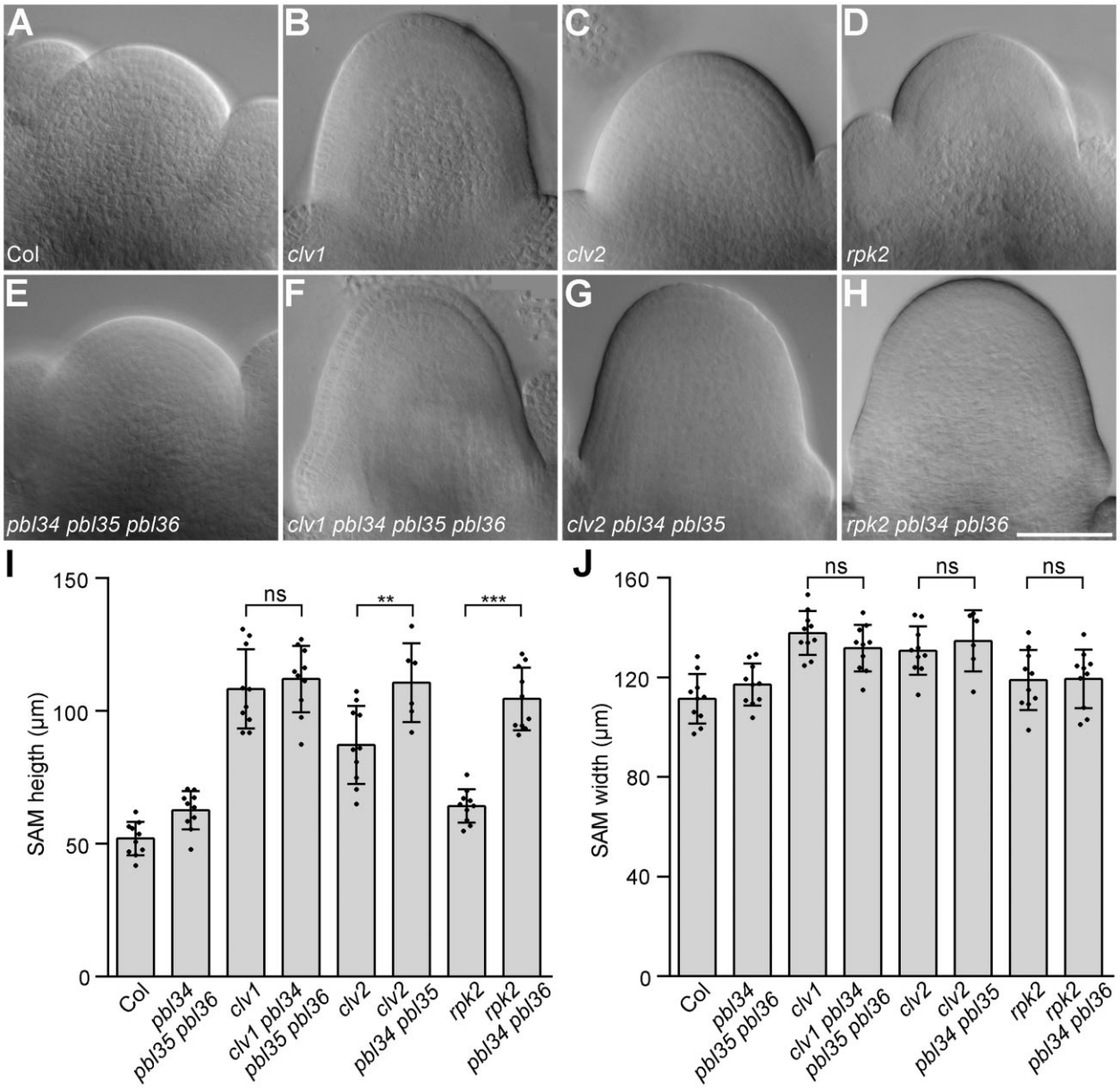

Figure 5 *pbl34 pbl35 pbl36* cannot enhance the SAM defects of *clv1*. A–H, DIC images of SAMs from 19-day-old seedlings of Col (A), *clv1* (B), *clv2* (C), *rpk2* (D), *pbl34 pbl35 pbl36* (E), *clv1 pbl34 pbl35 pbl36* (F), *clv2 pbl34 pbl35* (G), and *rpk2 pbl34 pbl36* (H). Scale bar: 50 μm. I, J, Quantitative analysis of SAM height (I) and width (J). Data are shown as mean ± SD (n = 10 independent plants). ***$P < 0.001$, **$P < 0.01$, ns represents no significant difference (two-tailed Student's t test).

also showed that PBL34/35 interact with CLV1, BAM3, and CIK1/2 (Figure 7B).

Stable double transgenic plants harboring PBL-Flag and CLV1-GFP, or PBL-Flag and BAM3-GFP, or PBL-GFP and CIK1-Flag were further used for co-immunoprecipitation (co-IP) assays. Consistent with the above results, PBL34/35 interact with CLV1, BAM3, and CIK1 in vivo. However, the interactions between PBL34/35 and CLV1, BAM3, or CIK1 in planta cannot be enhanced by CLV3 or CLE45 treatment (Figure 7C). Taken together, these results demonstrate that PBL34/35/36 associate with the CLV–CIK complex to control SAM homeostasis, and with the BAM–CIK complex to control proximal root meristem homeostasis.

PBL34/35 can be phosphorylated by CLV1 and BAM1 *in vitro*

Our previous work demonstrated that the CLV3 and CLE25/26/45 signals are transmitted through phosphorylation (Hu et al., 2018, 2022). Therefore, we speculated that PBL34/35/36 might be phosphorylated by CLV1, BAMs, or CIKs directly. In vitro kinase assays using recombinant proteins purified from *Escherichia coli* were performed to determine whether PBL34/35 can be phosphorylated by CLV1, BAMs, or CIKs. As we unable to obtain the fusion protein of the BAM3 cytoplasmic domain, the cytoplasmic domain of CLV1, BAM1, and CIK1/2 was used (Shimizu et al., 2015). Immunoblotting assays using an α-pThr antibody revealed that GST-CLV1$_{CD}$, GST-BAM1$_{CD}$,

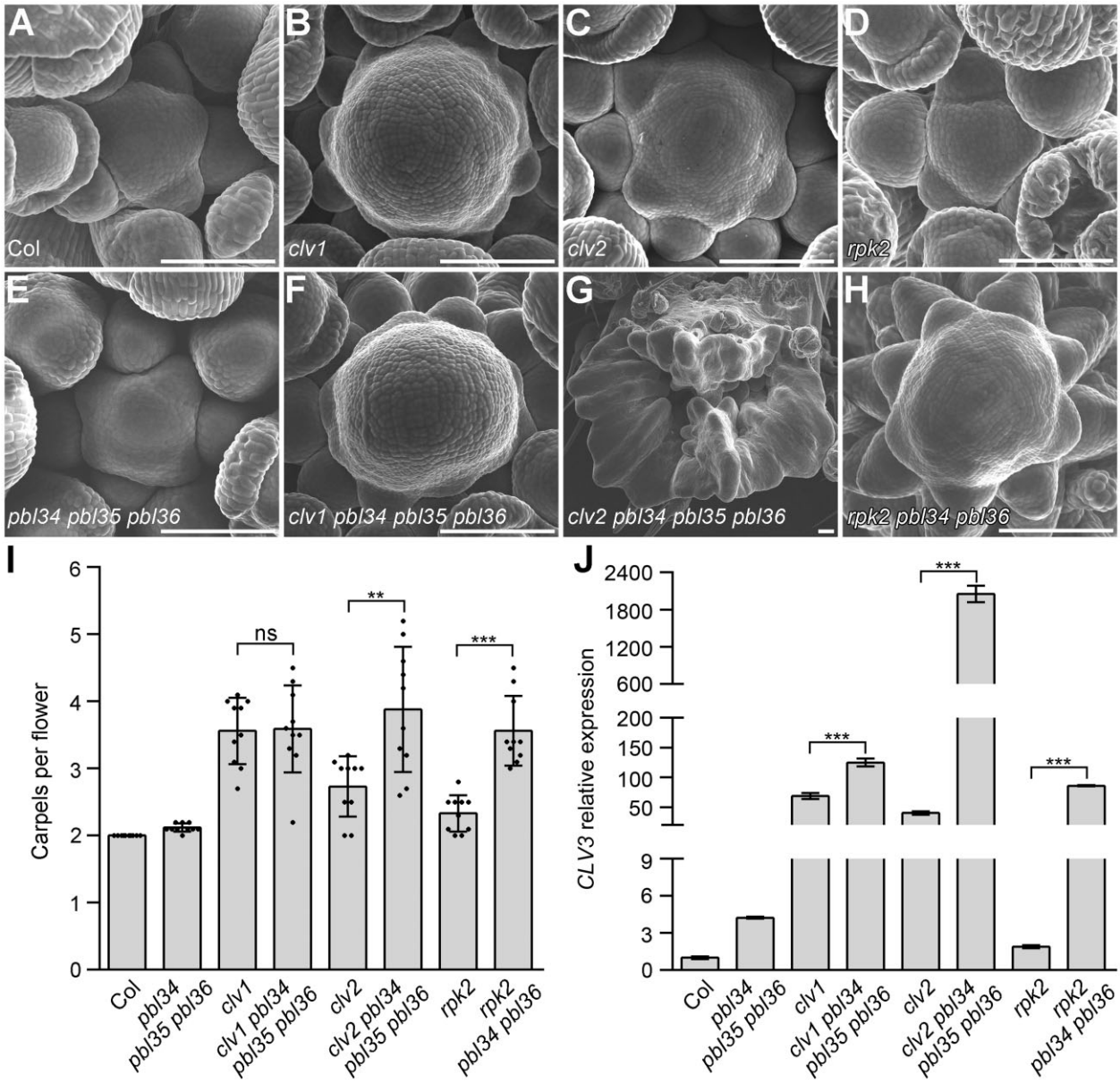

Figure 6 PBL34/35/36 function in the CLV1 pathway to transduce the CLV3 signal. A–H, SEM images of IMs in Col (A), *clv1* (B), *clv2* (C), *rpk2* (D), *pbl34 pbl35 pbl36* (E), *clv1 pbl34 pbl35 pbl36* (F), *clv2 pbl34 pbl35 pbl36* (G), and *rpk2 pbl34 pbl36* (H). Scale bars: 100 μm. I, Quantitative analyses of carpels per flower of the indicated genotypes. Data are shown as mean ± SD (n = 10 independent plants; each sample represents the average carpel number of each plant.). ***$P < 0.001$, **$P < 0.01$, ns represents no significant difference (two-tailed Student's t test). J, Relative expression of *CLV3* in the indicated genotypes was quantified by RT-qPCR. Data are shown as mean ± SD (n = 3 technical replicates, two biological replicates showed similar results). ***$P < 0.001$ (two-tailed Student's t test).

GST-CIK1$_{CD}$, and GST-CIK2$_{CD}$ possess strong autophosphorylation activities, whereas GST-mCLV1$_{CD}$, GST-mBAM1$_{CD}$, MBP-mPBL34$_{CD}$, and MBP-mPBL35$_{CD}$, in which a conserved lysine residue involved in ATP binding in their kinase domain was mutated, do not show any detectable autophosphorylation activities. It is apparent that GST-CLV1$_{CD}$ and GST-BAM1$_{CD}$ can directly phosphorylate MBP-mPBL34$_{CD}$ and MBP-mPBL35$_{CD}$, but GST-CIK1$_{CD}$ and GST-CIK2$_{CD}$ cannot (Figure 8). These data indicate that PBL34/35 act as direct substrates of CLV1 and BAM1/3 to maintain homeostasis of the SAM and RAM.

Discussion

PBL34/35/36 function directly downstream of BAM1/3 to control CLE25/26/45-mediated proximal root meristem maintenance and protophloem differentiation

RLCKs act as essential players in RLK-mediated signaling pathways to connect the activated RLKs with downstream signaling components in a variety of plant defense responses and growth processes (Liang and Zhou, 2018). Although BAM1/3 and CIKs were found to be

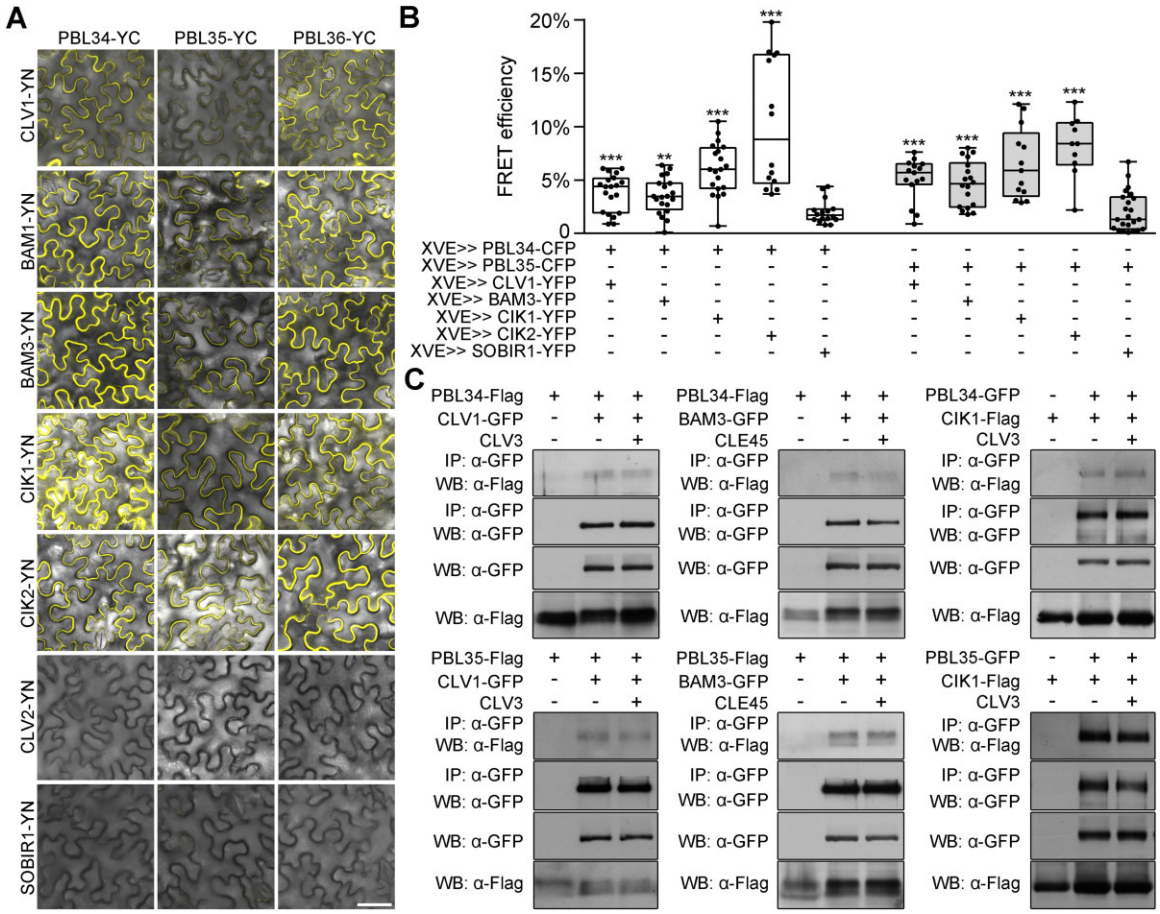

Figure 7 PBL34/35/36 interact with CLV1, BAM1/3, and CIKs. A, BiFC assay in *N. benthamiana* leaves to show interactions between PBL34/35/36 and CLV1, BAM1, BAM3, CIK1, CIK2, CLV2, and SOBIR1. PBLs were fused to the C-terminal part of YFP; CLV1, BAM1, BAM3, CIK1, CIK2, CLV2, and SOBIR1 were fused to the N-terminal part of YFP. Scale bar: 50 μm. B, Interactions of PBL34/35 with CLV1, BAM3, CIK1, CIK2, and SOBIR1 were detected by FRET in *N. benthamiana* leaves. All these proteins were transiently expressed under the control of the XVE≫oLexA-35S estradiol-inducible system. The FRET efficiencies between PBL34/35 and CLV1, BAM3, or CIKs were significantly higher than those with the control SOBIR1. Box limits indicate 25th and 75th percentiles; horizontal line is the median; whiskers display minimum and maximum values. Dots represent individual measurements from 10 to 23 samples per group. $^{***}P < 0.001$, $^{**}P < 0.01$ (two-tailed Student's *t* test). C, In vivo co-IP of PBL34/35-Flag and CIK1-Flag by CLV1/BAM3-GFP or PBL34/35-GFP, respectively, in stable transgenic plants. Ten-day-old stable transgenic seedlings harboring PBL34/35-Flag CLV1/BAM3-GFP or CIK1-Flag PBL34/35-GFP were harvested for protein extraction after treatment with or without 10-μM CLV3 or CLE45 for 10 min. Protein extracts were immunoprecipitated with an α-GFP antibody (IP: α-GFP), and then immunoblotted with an α-Flag (WB: α-Flag) or an α-GFP antibody (WB: α-GFP). Protein extracts before immunoprecipitation were immunoblotted with either α-Flag or α-GFP antibody as input.

involved in proximal root meristem maintenance and protophloem differentiation (Depuydt et al., 2013; Anne et al., 2018; Ren et al., 2019; Hu et al., 2022), the direct downstream effectors of the BAM–CIK complex in this process have not been identified. Here, we show that the root length, proximal root meristem, and protophloem of the *pbl34 pbl35 pbl36* triple mutants are resistant to the root-active CLE peptides (Figures 1 and 2; Supplemental Figures S4 and S6). Similar results were recently reported in a bioRxiv preprint (DeFalco et al., 2021). Genetic analysis also revealed that *bam3 pbl34 pbl35 pbl36* and *cik2 pbl34 pbl35 pbl36* do not show any additive defects when compared with *bam3*, *cik2*, and *pbl34 pbl35 pbl36* (Supplemental Figure S7). Further biochemical assays show that PBL34/35/36 interact with BAM1/3 and CIKs both in vivo and in vitro (Figure 7). These results demonstrate that PBL34/35/36 act downstream of BAM1/3 and CIKs, which mediate CLE signaling to regulate the proximal root meristem and protophloem differentiation.

However, the loss-of-function of *PBL34/35/36* can only slightly rescue the short-root phenotype of *brx* and *ops* (Supplemental Figure S8), which may be caused by the functional redundancy of PBL homologs. A similar scenario was found for *cik2*, which is partially resistant to all the root-active CLE peptides, but cannot suppress the root defects of *brx*, and can only slightly rescue the root defects of *ops*. Furthermore, the *cik2 cik3 cik4 cik5 cik6* mutation largely rescues the root defects of both *brx* and *ops* (Anne et al., 2018; Ren et al., 2019; Hu et al., 2022). Therefore, in *brx pbl34*

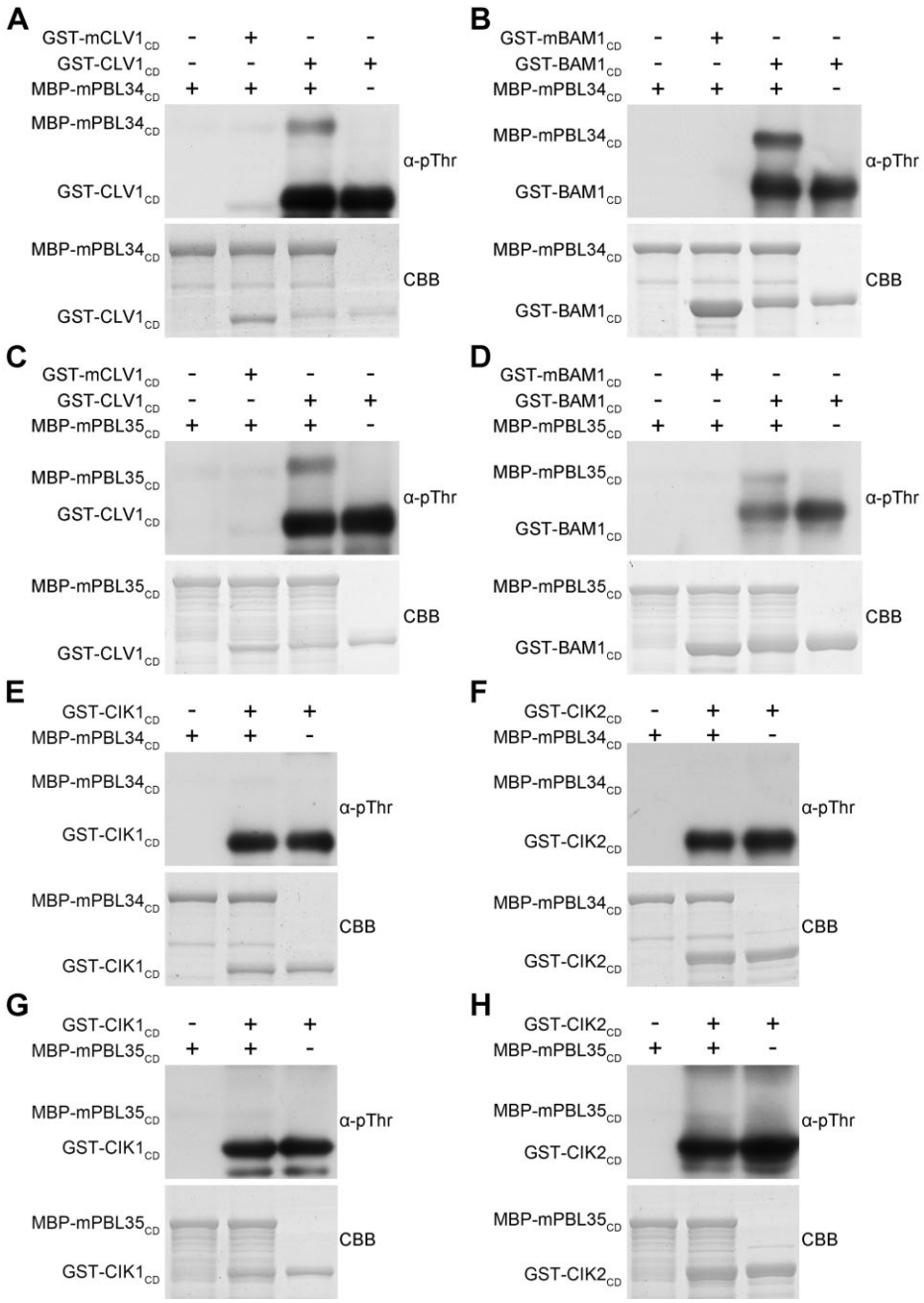

Figure 8 CLV1 and BAM1 phosphorylate PBL34 and PBL35 in vitro. A–H, In vitro kinase assays were performed by incubating GST-CLV1$_{CD}$ or GST-mCLV1$_{CD}$, GST-BAM1$_{CD}$ or GST-mBAM1$_{CD}$, GST-CIK1$_{CD}$ or GST-mCIK1$_{CD}$, and GST-CIK2$_{CD}$ or GST-mCIK2$_{CD}$ with MBP-mPBL34$_{CD}$ or MBP-mPBL35$_{CD}$, respectively. The phosphorylation levels were detected by α-pThr antibody. CBB, Coomassie brilliant blue staining.

pbl35 pbl36 and *ops pbl34 pbl35 pbl36*, other PBL members may compensate for the loss-of-function of PBL34/35/36 to transduce CLE signals. Generating and analyzing higher-order *pbl* mutants may provide insight into this possibility.

Interestingly, although PBL34/35/36 interact with both BAMs and CIKs, they can only be phosphorylated by BAM1, but not by CIKs in vitro (Figure 8). These results indicate that PBL34/35/36 may function as the direct substrates of BAMs to transduce CLE signals from the cell surface into the cytoplasm. Similarly, BSKs are the direct phosphorylation substrates of BRI1 to activate the downstream BR signaling components, whereas BSKs cannot be phosphorylated by BAK1 although BAK1 shows dramatically enhanced phosphorylation levels upon BR perception (Wang et al., 2005; Tang et al., 2008). Plants may employ a similar strategy by forming an RLK–RLCK complex that transduces extracellular signals into the cytoplasm.

PBL34/35/36 exhibit the CLV1 pathway-specific function to maintain SAM homeostasis

The SAM and RAM are evolutionarily related structures, and they employ several common or related regulators to

maintain stem cell niches. CLV1 is involved in regulating both SAM and the distal root meristem (Clark et al., 1997; Stahl et al., 2013); CLV2 and CRN are required to maintain the homeostasis of both the SAM and proximal root meristem (Kayes and Clark, 1998; Müller et al., 2008; Hazak et al., 2017); CIKs function redundantly in all these meristems (Hu et al., 2018; Zhu et al., 2021). In this study, our findings indicate that PBL34/35/36 also function as conserved regulators in both the SAM and RAM.

The *pbl34 pbl35 pbl36* mutants exhibit enlarged SAMs relative to the wild-type plants (Figure 3), and show reduced sensitivity to exogenously applied CLV3 (Figure 4; Supplemental Figure S10). Genetic analysis shows that additional mutations of *PBL34/35/36* greatly enhance the phenotype of *clv2* and *rpk2*, but not *clv1*, suggesting that PBL34/35/36 function in the CLV1 pathway, and act independently of CLV2 and RPK2 in maintaining SAM homeostasis. Biochemical assays show that PBL34/35/36 interact with CLV1 and CIKs both in vivo and in vitro, and they can be phosphorylated by CLV1, but not by CIKs in vitro, which is similar to the scenario that is found in PBL34/35/36-regulated RAM maintenance. The current findings support the notion that PBL34/35/36 may specifically act downstream of CLV1 in mediating the CLV3 signal to regulate SAM homeostasis.

We noticed that the *pbl34 pbl35 pbl36* mutant exhibits weaker SAM defects when compared with the *clv1*, *clv3*, and *cik* mutants (Figure 3; Hu et al., 2018). It is very possible that other PBL homologs also play a role in maintaining SAM homeostasis, similar to the situation found in PBL34/35/36-mediated RAM regulation. Alternatively, it cannot be ruled out that additional pathways parallel to PBL34/35/36 may also function downstream of CLV1 to mediate the CLV3 signal. Distinct effectors downstream of the same receptor may exist to transduce the same or different signals. For instance, FEA2 employs two different downstream effectors, CT2 (Gα) and ZmCRN, to maintain SAM homeostasis in maize by transducing the ZmFCP1 and ZmCLE7 signals, respectively (Je et al., 2018).

Potential applications of *PBL34/35/36* in agriculture

The CLV–WUS negative-feedback loop is conserved across angiosperms. Various *clv* mutants have been identified in rice (*Oryza sativa*), maize, and tomato (*Solanum lycopersicum*). The appropriately enlarged IMs and floral meristems of these *clv* mutants can result in more and bigger fruits (Somssich et al., 2016). Usually, strong *clv* mutants generate extremely flattened or split meristems, giving rise to very disorganized inflorescences that have poor seed yield, such as the null *td1* and *fea2* mutants in maize (Taguchi-Shiobara et al., 2001; Bommert et al., 2005). In contrast, meristems with slightly increased size in the weak *clv* mutants in crops will not lead to dramatically disorganized inflorescences, such as the weak alleles of *fea2*, *fea3*, *Zmcle7*, *Zmfcp1*, and *Zmcle1e5* mutants in maize, and can significantly improve crop productivity (Bommert et al., 2013a; Je et al., 2016; Liu et al., 2021). Actually, the homologs of PBL34/35/36 are widely spread in various species. Loss-of-function of *BnaA09g22690D* and *BnaA09g22670D*, two homologs of *PBL34/35/36* in *Brassica napus*, results in a fasciated stem, ultrahigh branching, and more flowers (Li et al., 2020), suggesting that PBLs possess conserved functions in maintaining SAM homeostasis across species. As *pbl34 pbl35 pbl36* is a weak mutant of the CLV signaling pathway, these three genes, and possibly their potential homologs, are appropriate candidate targets that can be used in modern breeding to improve crop productivity.

High-yield breeding requires not only good yield traits but also proper tolerance to various stresses since plants constantly cope with adverse environments. In general, turning on defense signaling often leads to decreased growth and yield, and turning off defense signaling will result in infected plants by pathogens. This defense–growth tradeoff is the biggest challenge for modern crop breeding (Wu et al., 2020). Therefore, a comprehensive understanding of the cross-talk between developmental and immune signaling is critical for providing essentially basic knowledge to maximize crop productivity. In addition to the functions in RAM and SAM discussed in this study, PBL34/35/36 have also been demonstrated to be downstream signaling components of LORE that recognizes medium-chain 3-hydroxy fatty acids in the plant immune response (Luo et al., 2020), indicating that PBL34/35/36 act as critical regulators in both SAM maintenance and the immune response. Therefore, PBL34/35/36 have the potential to balance the trade-off between defense response and development of inflorescences, branches, and flowers to improve crop productivity. Especially, the differentially phosphorylated sites of PBL34/35/36 by LORE and CLV1 may be engineered as potential targets to improve crop yield, but not affect the immune response.

Briefly, the results presented in this report demonstrate that CLV1- and BAM1/3-mediated CLE peptide signaling in the SAM and RAM require PBL34/35/36 functioning as downstream components to transduce the signals into the cytoplasm. Our findings not only provide essential insights into the molecular mechanisms controlling meristem homeostasis but also further substantiate the conservative strategy employed by RLK-mediated signaling pathways. In addition, *pbl34 pbl35 pbl36* mutants show reduced sensitivity to all of those CLE peptides that can consume the proximal root meristem, suggesting that PBL34/35/36 probably mediate multiple CLE signals to regulate plant growth and development.

Materials and methods

Plant materials and growth conditions

Arabidopsis (*Arabidopsis thaliana*) ecotype Columbia-0 (Col), various mutants, and transgenic plants in the Col background were used in this study. The T-DNA insertion lines, including *pbl34-1* (SALK_067743), *pbl34-2* (SALK_126209), *pbl35-1* (SALK_039402), *pbl36-1* (SAIL_885_B03), *pbl36-2* (SALK_074901), *pbl36-3* (SALK_058890), *bam3*

(SALK_044433), *cik2* (SALK_066568), *clv1-20* (SALK_008670), *clv2-101* (GK686A09), *rpk2-1* (SALK_062412), and *wus-101* (GK870H12), were obtained from the Arabidopsis Biological Resource Center (ABRC). *brx-2* and *ops-1* were used in previous studies (Li et al., 2009; Truernit et al., 2012). The *pbl34-3*, *pbl35-2*, and *pbl35-3* mutants were generated by CRISPR/Cas9-based gene editing (Wang et al., 2015). The corresponding single guide RNA (sgRNA) sequences are listed in Supplemental Table S1. The *pbl34-1*, *pbl35-1*, and *pbl36-1* mutants were used to generate the corresponding *pbl* double mutants and the *pbl34 pbl35 pbl36-1* triple mutant, which were employed for physiological and genetic analysis. The *pbl34 pbl35 pbl36-1* triple mutant was named *pbl34 pbl35 pbl36* for brevity in the text. The *pbl34-2*, *pbl35-2*, and *pbl36-2* mutants were used to create the *pbl34 pbl35 pbl36-2* mutant. The *pbl34 pbl35 pbl36-3* mutant was generated by crossing the *pbl34-3*, *pbl35-3*, and *pbl36-3* mutants. Seeds were sown in the soil after vernalization at 4°C for 3 days and then cultivated in a greenhouse with 16-h light at 20°C–22°C until the plants were used. For seedling analysis, surface-sterilized seeds were vernalized for 3 days and grown on half-strength MS medium plates containing 1% (w/v) sucrose and 0.8% (w/v) agar in a growth chamber with 16-h light (120 μmol s^{-1} m^{-2} light intensity provided by white LED lamps) and 8-h dark at 22°C. Peptide assays were performed as described previously (Hu et al., 2018; Zhu et al., 2021).

Phylogenetic analysis

Amino acid sequences of PBL34/35/36 and BIK1 were downloaded from The Arabidopsis Information Resource. The multiple sequence alignment was performed using MEGA6 (https://www.megasoftware.net). The phylogenetic tree was constructed using the neighbor-joining method with 1,000 bootstrap replicates. The evolutionary distances were computed using the Poisson correction method, and are in the units of the number of amino acid substitutions per site.

Creation of constructs and transgenic plants

To analyze the expression patterns of *PBL34/35/36*, the genomic fragments that encompass the promoter sequence and the coding sequence without the stop codon of each *PBL* were cloned into the *pBIB-BASTA-GWR-YFP* vector. To analyze protophloem differentiation, the promoters of *CVP2* and *APL* (Bonke et al., 2003; Scacchi et al., 2010) were cloned into the *pFYTAG* destination vector (Zhang et al., 2005) using Gateway technology.

The coding sequences of *PBL34/35/36*, *CIK1*, *CLV1*, and *BAM3* were cloned into the *pUBQ10-GWR-Flag* and *pH35GWG* destination vectors using Gateway technology. Double transgenic plants expressing *PBL-Flag* and *CLV1/BAM3-GFP* or *PBL-GFP* and *CIK1-Flag* were then generated for co-IP analyses. All transgenic plants were generated by the floral dip method (Clough and Bent, 1998) using the *Agrobacterium tumefaciens* GV3101 strain.

For BiFC assays, PBL34/35/36 were fused with the C-terminal part of YFP (YC) in the *pEarleygate201-YC* vector, and CLV1, BAM1, BAM3, CIK1, CIK2, CLV2, and SOBIR1 were fused with the N-terminal part of YFP (YN) in the *pEarleygate202-YN* vector (Lu et al., 2010b).

For FRET analyses with inducible vectors, PBL34/35 were fused with CFP in the *pER8-CFP* vector, and CLV1, BAM3, CIK1, CIK2, and SOBIR1 were fused with YFP in the *pER8-YFP* vector. Both *pER8-CFP* and *pER8-YFP* were modified by adding CFP or YFP into the binary destination vector *pER8* (Zuo et al., 2000) that was linearized by XhoI and SpeI. The Gateway cassette and CFP/YFP were amplified from *pBIB-BASTA-GWR-CFP/YFP*.

For protein purification, the kinase-inactive cytoplasmic domains of PBL34/35 were fused with an N-terminal MBP-tag using the *pMal-cRi* vector, and the wild-type or kinase-inactive cytoplasmic domains of CLV1, BAM1, CIK1, and CIK2 were fused with an N-terminal GST tag using the *pDEST15* vector.

Phenotypic analysis

The siliques were examined under a dissection microscope to count carpel number. The carpel number of each genotype was determined by averaging the number of carpels from 10 plants. The carpel number of each plant was determined by averaging carpel numbers from 20 or all siliques of the plant. For SAM analysis, leaves of 19-day-old seedlings were removed to expose the SAM under a dissection microscope, then the SAM was cleared in a mixture of chloral hydrate, glycerol, and water (4:1:2, w/v/v) on a glass slide for several minutes. Differential interference contrast (DIC) images of the SAM were taken using a microscope (Leica DM6000B) equipped with a DFC420C digital camera. The base of the SAM was defined as the location of leaf primordium, and the distance from the top of a SAM to the base was measured as the height. To observe the IM, flowers were removed from the inflorescence to expose the IM. The prepared samples were stuck to the stage of a microscope and were then frozen in liquid nitrogen for about 30 s (keeping the samples above the liquid nitrogen). The samples were subsequently examined by a Hitachi 4700 scanning electron microscope.

Microscopy analysis

PI staining and mPS-PI assays were performed as described previously (Zhu et al., 2021). Samples were observed and photographed using a confocal laser scanning microscope (LSM-880, ZEISS and A1R + Ti2-E, Nikon). Confocal imaging of fluorescence reporters in the IM of living plants was performed by using a Nikon (A1R + Ti2-E) confocal microscope. NIS-Elements AR (Nikon software) was used to reconstruct the Z-stacks for a longitudinal view. To image the YFP and PI signals simultaneously in the IM, the multi-tracking mode of the Nikon confocal microscope was used. YFP was excited at 487 nm and the signals at 500–550 nm were collected. PI was excited using a 560 nm laser and the signals at 570–620 nm were collected.

FRET experiments were conducted using a Zeiss LSM 880. CFP donor fluorophores were excited at 458 nm, and the

signals were collected at 463–510 nm. YFP acceptor fluorophores were excited at 514 nm, and the signals were collected at 520–620 nm. To perform acceptor photobleaching, the selected regions of interest were photobleached by defined parameters. The prebleach and postbleach images were collected, and the fluorescence intensity of CFP and YFP were recorded before and after photobleaching.

RNA in situ hybridization and quantitative reverse transcription polymerase chain reaction (qRT-PCR)

RNA *in situ* hybridization of *CLV3* and *WUS* was performed as described previously (Hu et al., 2018). Total RNA of Col, *pbl34 pbl35 pbl36*, *clv1*, *clv1 pbl34 pbl35 pbl36*, *clv2*, *clv2 pbl34 pbl35 pbl36*, *rpk2*, and *rpk2 pbl34 pbl36* was extracted from 5-week-old IMs with young flowers using an RNA extraction kit (TIANGEN, DP432). Five micrograms of total RNA of each sample was used to synthesize cDNA using HiScript II Q RT SuperMix (Vazyme Biotech, R223). Quantitative RT-PCR analysis was performed with a StepOnePlus Real-time PCR System (Applied Biosystems) using Hieff qPCR SYBR Green Master Mix (YEASEN, 11203ES03) to examine the relative expression of *CLV3*. Primers used in this study are listed in Supplemental Table S1.

Biochemical assays

BiFC, mbSUS yeast two-hybrid, co-IP, and in vitro phosphorylation assays were performed as described previously (Cui et al., 2018; Hu et al., 2018). Commercial antibodies of Flag (α-Flag; Abmart, M20008L, lot 334077; 1:3,000 dilution), GFP (α-GFP; Roche; 11814460001, lot 47859600; 1:3,000 dilution), and phosphothreonine (α-pThr; Cell Signaling Technology; 9381, lot 25; 1:2,500 dilution) were used for immunoblot analyses. For the mbSUS yeast two-hybrid assay, full-length coding sequences of *PBL34*, *PBL35*, and *PBL36* were co-transferred into the yeast strain THY.AP5 with the vector *pX-NubWTgate* linearized by EcoRI and SmaI, and full-length coding sequences of *CLV1*, *BAM3*, *CIK1*, *CIK2*, and *SOBIR1* were co-transferred into the yeast strain THY.AP4 with the vector *pMetYCgate* linearized by PstI and HindIII.

For isolating mesophyll protoplasts of *N. benthamiana*, the infiltrated leaves were cut into small pieces and then incubated with 5-mL protoplast Enzyme Solution (1.5% [w/v] cellulase R10, and 0.4% [w/v] macerozyme R10, 0.4-M mannitol, 20-mM KCl, 20-mM MES, pH 5.7, 10-mM $CaCl_2$, 1.83-μL 2-mercaptoethanol, 0.1% [w/v] BSA) in a vacuum for 30 min. The samples were then transferred into darkness for 4 h with gentle shaking. After an equal volume of W5 Solution (2-mM MES, pH 5.7, 154-mM NaCl, 125-mM $CaCl_2$, 5-mM KCl) was added to each sample, the precipitates were collected by centrifuging at 100*g* for 2 min at room temperature and then resuspended with 0.5-mL washing and incubation solution (0.5-M mannitol, 4-mM MES, pH 5.7, 20-mM KCl).

For inducible FRET, the transiently transformed *N. benthamiana* leaves under the control of an estradiol-inducible promoter (Zuo et al., 2000) were grown for 36 h and then sprayed with 20-μM β-estradiol 6 h prior to imaging. The FRET efficiencies were quantified by measuring the intensity increase of the donor fluorophore (CFP) after bleaching of the acceptor according to the following formula (Weidtkamp-Peters and Stahl, 2017):

$$\text{FRET efficiency} = (\text{Intensity}_{\text{Donor after}} - \text{Intensity}_{\text{Donor before}})/\text{Intensity}_{\text{Donor after}} \times 100$$

For protein purification, the expression of MBP-tagged kinase-inactive cytoplasmic domains of PBL34/35 was induced with 0.2-mM IPTG for 6 h at 28°C and the expression of GST-tagged cytoplasmic domains of CLV1, BAM1, CIK1, and CIK2 was induced with 0.2-mM IPTG for 16 h at 18°C.

Quantification and statistical analysis

Data for quantification analyses are presented as mean ± SD. Statistical analyses were performed using GraphPad Prism software (version 6.0) and Microsoft Excel 2010. Results of all statistical analyses are presented in Supplemental Data Set S2.

Accession numbers

Sequence data from this article can be found in the Arabidopsis TAIR database (www.arabidopsis.org) under the following accession numbers: APL (AT1G79430), BAM1 (AT5G65700), BAM3 (AT4G20270), BRX (AT1G31880), CIK1 (AT1G60800), CIK2/CLERK (AT2G23950), CLE25 (AT3G28455), CLE45 (AT1G69588), CLV1 (AT1G75820), CLV2 (AT1G65380), CLV3 (AT2G27250), CVP2 (AT1G05470), OPS (AT3G09070), PBL34 (AT5g15080), PBL35 (AT3G01300), PBL36 (AT3g28690), RPK2 (AT3G02130), SOBIR1 (AT2G31880), WUS (AT2G17950).

Supplemental data

The following materials are available in the online version of this article.

Supplemental Figure S1. *pbl34* is less sensitive to CLE45 treatment.

Supplemental Figure S2. *PBL34/35/36* are expressed in the RAM.

Supplemental Figure S3. Gene structures of *PBL34/35/36* and location of T-DNA insertions and CRISPR/Cas9-mediated mutations.

Supplemental Figure S4. PBL34/35/36 are required for CLE45-mediated proximal root meristem consumption.

Supplemental Figure S5. Complementation of *PBL34/35/36* can rescue the defects of *pbl34 pbl35 pbl36*.

Supplemental Figure S6. *pbl34 pbl35 pbl36* showed resistance to root-active CLEs.

Supplemental Figure S7. PBL34/35/36 function in a common pathway with BAM3 and CIK2.

Supplemental Figure S8. *pbl34 pbl35 pbl36* partially rescues the short root of *brx* and *ops*.

Supplemental Figure S9. *PBL34/35/36* are expressed in the SAM.

Supplemental Figure S10. PBL34/35/36 are involved in the CLV3-mediated signaling pathway.

Supplemental Figure S11. *pbl34 pbl35 pbl36* and *pbl34 pbl36* enhance the phenotype of *clv2* and *rpk2*, respectively.

Supplemental Figure S12. PBL34/35/36 interact with CLV1, BAM3, CIK1, and CIK2 on the plasma membrane.

Supplemental Table S1. Primers used in this study.

Supplemental Data Set S1. Alignments used to generate the phylogeny presented in Supplemental Figure S1B.

Supplemental Data Set S2. Summary of statistical analyses.

Acknowledgments

We thank the ABRC for the T-DNA insertion lines used in this study. We thank Dr. Jun Liu (Institute of Microbiology, Chinese Academy of Sciences) for nicely providing us with the MBP-mPBL34$_{CD}$ construct. We are grateful to Dr Chun-Ming Liu (Peking University) for kindly providing us with the *brx-2* and *ops-1* mutants. We are grateful to Ms Liang Peng, Ms Haiyan Li, Ms Liping Guan, Dr Yahu Gao, and Dr Yang Zhao (Core Facility for Life Science Research, Lanzhou University) for technical assistance.

Funding

This work was supported by National Natural Science Foundation of China (31970339, 32170332, 31770312, 31900166, and 32000594), the 111 Project (B16022), China Postdoctoral Science Foundation (BX20180133), Fundamental Research Funds for the Central Universities (lzujbky-2021-kb05, lzujbky-2022-kb05), and Lanzhou City's Scientific Research Funding Subsidy to Lanzhou University.

Conflict of interest statement. The authors declare no competing interests.

References

Anne P, Amiguet-Vercher A, Brandt B, Kalmbach L, Geldner N, Hothorn M, Hardtke CS (2018) CLERK is a novel receptor kinase required for sensing of root-active CLE peptides in Arabidopsis. Development **145**: dev162354

Betsuyaku S, Sawa S, Yamada M (2011a) The function of the CLE peptides in plant development and plant-microbe interactions. Arabidopsis Book **9**: e0149

Betsuyaku S, Takahashi F, Kinoshita A, Miwa H, Shinozaki K, Fukuda H, Sawa S (2011b) Mitogen-activated protein kinase regulated by the CLAVATA receptors contributes to shoot apical meristem homeostasis. Plant Cell Physiol **52**: 14–29

Bleckmann A, Weidtkamp-Peters S, Seidel CA, Simon R (2010) Stem cell signaling in Arabidopsis requires CRN to localize CLV2 to the plasma membrane. Plant Physiol **152**: 166–176

Blümke P, Schlegel J, Gonzalez-Ferrer C, Becher S, Pinto KG, Monaghan J, Simon R (2021) Receptor-like cytoplasmic kinase MAZZA mediates developmental processes with CLAVATA1-family receptors in Arabidopsis. J Exp Bot **72**: 4853–4870

Boisson-Dernier A, Franck CM, Lituiev DS, Grossniklaus U (2015) Receptor-like cytoplasmic kinase MARIS functions downstream of CrRLK1L-dependent signaling during tip growth. Proc Natl Acad Sci USA **112**: 12211–12216

Bommert P, Nagasawa NS, Jackson D (2013a) Quantitative variation in maize kernel row number is controlled by the *FASCIATED EAR2* locus. Nat Genet **45**: 334–337

Bommert P, Je BI, Goldshmidt A, Jackson D (2013b) The maize Gα gene *COMPACT PLANT2* functions in CLAVATA signalling to control shoot meristem size. Nature **502**: 555–558

Bommert P, Lunde C, Nardmann J, Vollbrecht E, Running M, Jackson D, Hake S, Werr W (2005) *THICK TASSEL DWARF1* encodes a putative maize ortholog of the Arabidopsis CLAVATA1 leucine-rich repeat receptor-like kinase. Development **132**: 1235–1245

Bonke M, Thitamadee S, Mahonen AP, Hauser MT, Helariutta Y (2003) APL regulates vascular tissue identity in Arabidopsis. Nature **426**: 181–186

Brand U, Fletcher JC, Hobe M, Meyerowitz EM, Simon R (2000) Dependence of stem cell fate in Arabidopsis on a feedback loop regulated by CLV3 activity. Science **289**: 617–619

Breda AS, Hazak O, Schultz P, Anne P, Graeff M, Simon R, Hardtke CS (2019) A cellular insulator against CLE45 peptide signaling. Curr Biol **29**: 2501–2508

Burr CA, Leslie ME, Orlowski SK, Chen I, Wright CE, Daniels MJ, Liljegren SJ (2011) CAST AWAY, a membrane-associated receptor-like kinase, inhibits organ abscission in Arabidopsis. Plant Physiol **156**: 1837–1850

Clark SE, Williams RW, Meyerowitz EM (1997) The *CLAVATA1* gene encodes a putative receptor kinase that controls shoot and floral meristem size in Arabidopsis. Cell **89**: 575–585

Clough SJ, Bent AF (1998) Floral dip: a simplified method for *Agrobacterium*-mediated transformation of *Arabidopsis thaliana*. Plant J **16**: 735–743

Cui Y, Hu C, Zhu Y, Cheng K, Li X, Wei Z, Xue L, Lin F, Shi H, Yi J, et al. (2018). CIK receptor kinases determine cell fate specification during early anther development in Arabidopsis. Plant Cell **30**: 2383–2401

DeFalco TA, Anne P, James SR, Willoughby A, Johanndrees O, Genolet Y, Pullen A-M, Zipfel C, Hardtke CS, Nimchuk ZL (2021) A conserved regulatory module regulates receptor kinase signaling in immunity and development. bioRxiv preprint. doi: 10.1101/2021.01.19.427293 (January 20, 2021)

Depuydt S, Rodriguez-Villalon A, Santuari L, Wyser-Rmili C, Ragni L, Hardtke CS (2013) Suppression of Arabidopsis protophloem differentiation and root meristem growth by CLE45 requires the receptor-like kinase BAM3. Proc Natl Acad Sci USA **110**: 7074–7079

Deyoung BJ, Clark SE (2008) BAM receptors regulate stem cell specification and organ development through complex interactions with CLAVATA signaling. Genetics **180**: 895–904

Du C, Li X, Chen J, Chen W, Li B, Li C, Wang L, Li J, Zhao X, Lin J, et al. (2016). Receptor kinase complex transmits RALF peptide signal to inhibit root growth in Arabidopsis. Proc Natl Acad Sci USA **113**: 8326–8334

Fiers M, Golemiec E, Xu J, van der Geest L, Heidstra R, Stiekema W, Liu CM (2005) The 14-amino acid CLV3, CLE19, and CLE40 peptides trigger consumption of the root meristem in Arabidopsis through a CLAVATA2-dependent pathway. Plant Cell **17**: 2542–2553

Gallois JL, Nora FR, Mizukami Y, Sablowski R (2004) WUSCHEL induces shoot stem cell activity and developmental plasticity in the root meristem. Genes Dev **18**: 375–380

Gou X, Li J (2020) Paired receptor and coreceptor kinases perceive extracellular signals to control plant development. Plant Physiol **182**: 1667–1681

Gujas B, Kastanaki E, Sturchler A, Cruz TMD, Ruiz-Sola MA, Dreos R, Eicke S, Truernit E, Rodriguez-Villalon A (2020) A reservoir of pluripotent phloem cells safeguards the linear developmental trajectory of protophloem sieve elements. Curr Biol **30**: 755–766

Guo Y, Han L, Hymes M, Denver R, Clark SE (2010) CLAVATA2 forms a distinct CLE-binding receptor complex regulating Arabidopsis stem cell specification. Plant J **63**: 889–900

Hazak O, Brandt B, Cattaneo P, Santiago J, Rodriguez-Villalon A, Hothorn M, Hardtke CS (2017) Perception of root-active CLE peptides requires CORYNE function in the phloem vasculature. EMBO Rep **18**: 1367–1381

Hu C, Zhu Y, Cui Y, Cheng K, Liang W, Wei Z, Zhu M, Yin H, Zeng L, Xiao Y, et al. (2018) A group of receptor kinases are essential for CLAVATA signalling to maintain stem cell homeostasis. Nat Plants **4**: 205–211

Hu C, Zhu Y, Cui Y, Zeng L, Li S, Meng F, Huang S, Wang W, Kui H, Yi J, et al. (2022) A CLE-BAM-CIK signalling module controls root protophloem differentiation in Arabidopsis. New Phytol **233**: 282–296

Ishida T, Tabata R, Yamada M, Aida M, Mitsumasu K, Fujiwara M, Yamaguchi K, Shigenobu S, Higuchi M, Tsuji H, et al. (2014). Heterotrimeric G proteins control stem cell proliferation through CLAVATA signaling in Arabidopsis. EMBO Rep **15**: 1202–1209

Ito Y, Nakanomyo I, Motose H, Iwamoto K, Sawa S, Dohmae N, Fukuda H (2006) Dodeca-CLE peptides as suppressors of plant stem cell differentiation. Science **313**: 842–845

Je BI, Xu F, Wu Q, Liu L, Meeley R, Gallagher JP, Corcilius L, Payne RJ, Bartlett ME, Jackson D (2018) The CLAVATA receptor FASCIATED EAR2 responds to distinct CLE peptides by signaling through two downstream effectors. eLife **7**: e35673

Je BI, Gruel J, Lee YK, Bommert P, Arevalo ED, Eveland AL, Wu Q, Goldshmidt A, Meeley R, Bartlett M, et al. (2016). Signaling from maize organ primordia via FASCIATED EAR3 regulates stem cell proliferation and yield traits. Nat Genet **48**: 785–791

Kadota Y, Sklenar J, Derbyshire P, Stransfeld L, Asai S, Ntoukakis V, Jones JD, Shirasu K, Menke F, Jones A, et al. (2014) Direct regulation of the NADPH oxidase RBOHD by the PRR-associated kinase BIK1 during plant immunity. Mol Cell **54**: 43–55

Kayes JM, Clark SE (1998) CLAVATA2, a regulator of meristem and organ development in Arabidopsis. Development **125**: 3843–3851

Kim TW, Guan S, Burlingame AL, Wang ZY (2011) The CDG1 kinase mediates brassinosteroid signal transduction from BRI1 receptor kinase to BSU1 phosphatase and GSK3-like kinase BIN2. Mol Cell **43**: 561–571

Kinoshita A, Betsuyaku S, Osakabe Y, Mizuno S, Nagawa S, Stahl Y, Simon R, Yamaguchi-Shinozaki K, Fukuda H, Sawa S (2010) RPK2 is an essential receptor-like kinase that transmits the CLV3 signal in Arabidopsis. Development **137**: 3911–3920

Kitagawa M, Jackson D (2019) Control of meristem size. Annu Rev Plant Biol **70**: 269–291

Lee H, Jun YS, Cha OK, Sheen J (2019) Mitogen-activated protein kinases MPK3 and MPK6 are required for stem cell maintenance in the Arabidopsis shoot apical meristem. Plant Cell Rep **38**: 311–319

Li B, Gao J, Chen J, Wang Z, Shen W, Yi B, Wen J, Ma C, Shen J, Fu T, Tu J (2020) Identification and fine mapping of a major locus controlling branching in *Brassica napus*. Theor Appl Genet **133**: 771–783

Li J, Mo X, Wang J, Chen N, Fan H, Dai C, Wu P (2009) BREVIS RADIX is involved in cytokinin-mediated inhibition of lateral root initiation in Arabidopsis. Planta **229**: 593–603

Liang X, Zhou JM (2018) Receptor-like cytoplasmic kinases: central players in plant receptor kinase-mediated signaling. Annu Rev Plant Biol **69**: 267–299

Liao HZ, Zhu MM, Cui HH, Du XY, Tang Y, Chen LQ, Ye Z, Zhang XQ (2016) MARIS plays important roles in Arabidopsis pollen tube and root hair growth. J Integr Plant Biol **58**: 927–940

Liu L, Gallagher J, Arevalo ED, Chen R, Skopelitis T, Wu Q, Bartlett M, Jackson D (2021) Enhancing grain-yield-related traits by CRISPR-Cas9 promoter editing of maize *CLE* genes. Nat Plants **7**: 287–294

Liu Z, Wu Y, Yang F, Zhang Y, Chen S, Xie Q, Tian X, Zhou JM (2013) BIK1 interacts with PEPRs to mediate ethylene-induced immunity. Proc Natl Acad Sci USA **110**: 6205–6210

Lu D, Wu S, Gao X, Zhang Y, Shan L, He P (2010a) A receptor-like cytoplasmic kinase, BIK1, associates with a flagellin receptor complex to initiate plant innate immunity. Proc Natl Acad Sci USA **107**: 496–501

Lu Q, Tang X, Tian G, Wang F, Liu K, Nguyen V, Kohalmi SE, Keller WA, Tsang EW, Harada JJ, et al. (2010b). Arabidopsis homolog of the yeast *TREX-2* mRNA export complex: components and anchoring nucleoporin. Plant J **61**: 259–270

Luo X, Wu W, Liang Y, Xu N, Wang Z, Zou H, Liu J (2020) Tyrosine phosphorylation of the lectin receptor-like kinase LORE regulates plant immunity. EMBO J **39**: e102856

Mayer KF, Schoof H, Haecker A, Lenhard M, Jurgens G, Laux T (1998) Role of *WUSCHEL* in regulating stem cell fate in the Arabidopsis shoot meristem. Cell **95**: 805–815

Müller R, Bleckmann A, Simon R (2008) The receptor kinase CORYNE of Arabidopsis transmits the stem cell-limiting signal CLAVATA3 independently of CLAVATA1. Plant Cell **20**: 934–946

Nimchuk ZL, Zhou Y, Tarr PT, Peterson BA, Meyerowitz EM (2015) Plant stem cell maintenance by transcriptional cross-regulation of related receptor kinases. Development **142**: 1043–1049

Olsson V, Joos L, Zhu S, Gevaert K, Butenko MA, De Smet I (2019) Look closely, the beautiful may be small: precursor-derived peptides in plants. Annu Rev Plant Biol **70**: 153–186

Pandey S (2019) Heterotrimeric G-protein signaling in plants: conserved and novel mechanisms. Annu Rev Plant Biol **70**: 213–238

Perales M, Rodriguez K, Snipes S, Yadav RK, Diaz-Mendoza M, Reddy GV (2016) Threshold-dependent transcriptional discrimination underlies stem cell homeostasis. Proc Natl Acad Sci USA **113**: 6298–6306

Ranf S, Eschen-Lippold L, Frohlich K, Westphal L, Scheel D, Lee J (2014) Microbe-associated molecular pattern-induced calcium signaling requires the receptor-like cytoplasmic kinases, PBL1 and BIK1. BMC Plant Biol **14**: 374

Rao S, Zhou Z, Miao P, Bi G, Hu M, Wu Y, Feng F, Zhang X, Zhou JM (2018) Roles of receptor-like cytoplasmic kinase VII members in pattern-triggered immune signaling. Plant Physiol **177**: 1679–1690

Ren SC, Song XF, Chen WQ, Lu R, Lucas WJ, Liu CM (2019) CLE25 peptide regulates phloem initiation in Arabidopsis through a CLERK-CLV2 receptor complex. J Integr Plant Biol **61**: 1043–1061

Rodriguez-Villalon A, Gujas B, van Wijk R, Munnik T, Hardtke CS (2015) Primary root protophloem differentiation requires balanced phosphatidylinositol-4,5-biphosphate levels and systemically affects root branching. Development **142**: 1437–1446

Rodriguez-Villalon A, Gujas B, Kang YH, Breda AS, Cattaneo P, Depuydt S, Hardtke CS (2014) Molecular genetic framework for protophloem formation. Proc Natl Acad Sci USA **111**: 11551–11556

Rodriguez K, Perales M, Snipes S, Yadav RK, Diaz-Mendoza M, Reddy GV (2016) DNA-dependent homodimerization, sub-cellular partitioning, and protein destabilization control WUSCHEL levels and spatial patterning. Proc Natl Acad Sci USA **113**: 6307–6315

Scacchi E, Salinas P, Gujas B, Santuari L, Krogan N, Ragni L, Berleth T, Hardtke CS (2010) Spatio-temporal sequence of cross-regulatory events in root meristem growth. Proc Natl Acad Sci USA **107**: 22734–22739

Schoof H, Lenhard M, Haecker A, Mayer KFX, Jurgens G, Laux T (2000) The stem cell population of Arabidopsis shoot meristems is maintained by a regulatory loop between the *CLAVATA* and *WUSCHEL* genes. Cell **100**: 635–644

Shimizu N, Ishida T, Yamada M, Shigenobu S, Tabata R, Kinoshita A, Yamaguchi K, Hasebe M, Mitsumasu K, Sawa S (2015) BAM 1 and RECEPTOR-LIKE PROTEIN KINASE 2 constitute

a signaling pathway and modulate CLE peptide-triggered growth inhibition in Arabidopsis root. New Phytol **208**: 1104–1113

Shiu SH, Karlowski WM, Pan R, Tzeng YH, Mayer KF, Li WH (2004) Comparative analysis of the receptor-like kinase family in Arabidopsis and rice. Plant Cell **16**: 1220–1234

Somssich M, Je BI, Simon R, Jackson D (2016) CLAVATA-WUSCHEL signaling in the shoot meristem. Development **143**: 3238–3248

Song SK, Clark SE (2005) POL and related phosphatases are dosage-sensitive regulators of meristem and organ development in Arabidopsis. Dev Biol **285**: 272–284

Song SK, Lee MM, Clark SE (2006) POL and PLL1 phosphatases are CLAVATA1 signaling intermediates required for Arabidopsis shoot and floral stem cells. Development **133**: 4691–4698

Sreeramulu S, Mostizky Y, Sunitha S, Shani E, Nahum H, Salomon D, Hayun LB, Gruetter C, Rauh D, Ori N, et al. (2013) BSKs are partially redundant positive regulators of brassinosteroid signaling in Arabidopsis. Plant J **74**: 905–919

Stahl Y, Grabowski S, Bleckmann A, Kuhnemuth R, Weidtkamp-Peters S, Pinto KG, Kirschner GK, Schmid JB, Wink RH, Hulsewede A, et al. (2013) Moderation of Arabidopsis root stemness by CLAVATA1 and ARABIDOPSIS CRINKLY4 receptor kinase complexes. Curr Biol **23**: 362–371

Taguchi-Shiobara F, Yuan Z, Hake S, Jackson D (2001) The *FASCIATED EAR2* gene encodes a leucine-rich repeat receptor-like protein that regulates shoot meristem proliferation in maize. Genes Dev **15**: 2755–2766

Tang W, Kim TW, Oses-Prieto JA, Sun Y, Deng Z, Zhu S, Wang R, Burlingame AL, Wang ZY (2008) BSKs mediate signal transduction from the receptor kinase BRI1 in Arabidopsis. Science **321**: 557–560

Truernit E, Bauby H, Belcram K, Barthelemy J, Palauqui JC (2012) OCTOPUS, a polarly localised membrane-associated protein, regulates phloem differentiation entry in *Arabidopsis thaliana*. Development **139**: 1306–1315

Truernit E, Bauby H, Dubreucq B, Grandjean O, Runions J, Barthelemy J, Palauqui JC (2008) High-resolution whole-mount imaging of three-dimensional tissue organization and gene expression enables the study of Phloem development and structure in Arabidopsis. Plant Cell **20**: 1494–1503

Wang X, Goshe MB, Soderblom EJ, Phinney BS, Kuchar JA, Li J, Asami T, Yoshida S, Huber SC, Clouse SD (2005) Identification and functional analysis of *in vivo* phosphorylation sites of the Arabidopsis BRASSINOSTEROID-INSENSITIVE1 receptor kinase. Plant Cell **17**: 1685–1703

Wang Z, Gou X (2020) Receptor-like protein kinases function upstream of MAPKs in regulating plant development. Int J Mol Sci **21**: 7638

Wang ZP, Xing HL, Dong L, Zhang HY, Han CY, Wang XC, Chen QJ (2015) Egg cell-specific promoter-controlled CRISPR/Cas9 efficiently generates homozygous mutants for multiple target genes in Arabidopsis in a single generation. Genome Biol **16**: 144

Weidtkamp-Peters S, Stahl Y (2017) The use of FRET/FLIM to study proteins interacting with plant receptor kinases. Methods Mol Biol **1621**: 163–175

Wu Q, Xu F, Liu L, Char SN, Ding Y, Je BI, Schmelz E, Yang B, Jackson D (2020) The maize heterotrimeric G protein beta subunit controls shoot meristem development and immune responses. Proc Natl Acad Sci USA **117**: 1799–1805

Zhang C, Gong FC, Lambert GM, Galbraith DW (2005) Cell type-specific characterization of nuclear DNA contents within complex tissues and organs. Plant Methods **1**: 7

Zhang J, Li W, Xiang T, Liu Z, Laluk K, Ding X, Zou Y, Gao M, Zhang X, Chen S, et al. (2010). Receptor-like cytoplasmic kinases integrate signaling from multiple plant immune receptors and are targeted by a *Pseudomonas syringae* effector. Cell Host Microbe **7**: 290–301

Zhang Z, Liu L, Kucukoglu M, Tian D, Larkin RM, Shi X, Zheng B (2020) Predicting and clustering plant *CLE* genes with a new method developed specifically for short amino acid sequences. BMC Genomics **21**: 709

Zhu Y, Hu C, Gou X (2020) Receptor-like protein kinase-mediated signaling in controlling root meristem homeostasis. aBIOTECH **1**: 157–168

Zhu Y, Hu C, Cui Y, Zeng L, Li S, Zhu M, Meng F, Huang S, Long L, Yi J, et al. (2021). Conserved and differentiated functions of cik receptor kinases in modulating stem cell signaling in Arabidopsis. Mol Plant **14**: 1119–1134

Zuo J, Niu QW, Chua NH (2000) An estrogen receptor-based transactivator XVE mediates highly inducible gene expression in transgenic plants. Plant J **24**: 265–273